



Available online at www.sciencedirect.com

SciVerse ScienceDirect

Geochimica et Cosmochimica Acta 79 (2012) 106–126

Geochimica et
Cosmochimica
Acta

www.elsevier.com/locate/gca

Hydrogen isotope ratios of lacustrine sedimentary *n*-alkanes as proxies of tropical African hydrology: Insights from a calibration transect across Cameroon

Yannick Garcin^{a,*}, Valérie F. Schwab^b, Gerd Gleixner^b, Ansgar Kahmen^c, Gilbert Todou^d, Olivier Séné^e, Jean-Michel Onana^e, Gaston Achoundong^e, Dirk Sachse^a

^a DFG-Leibniz Center for Surface Process and Climate Studies, Institut für Erd- und Umweltwissenschaften, Universität Potsdam, Germany

^b Max-Planck-Institut für Biogeochemie, Jena, Germany

^c Institute of Agricultural Sciences, ETH Zurich, Switzerland

^d École Normale Supérieure, University of Maroua, Cameroon

^e National Herbarium of Cameroon, IRAD, Yaoundé, Cameroon

Received 3 May 2011; accepted in revised form 22 November 2011; available online 1 December 2011

Abstract

Hydrogen isotope values (δD) of sedimentary aquatic and terrestrial lipid biomarkers, originating from algae, bacteria, and leaf wax, have been used to record isotopic properties of ancient source water (i.e., precipitation and/or lake water) in several mid- and high-latitude lacustrine environments. In the tropics, however, where both processes associated with isotope fractionation in the hydrologic system and vegetation strongly differ from those at higher latitudes, calibration studies for this proxy are not yet available. To close this gap of knowledge, we sampled surface sediments from 11 lakes in Cameroon to identify those hydro-climatological processes and physiological factors that determine the hydrogen isotopic composition of aquatic and terrestrial lipid biomarkers. Here we present a robust framework for the application of compound-specific hydrogen isotopes in tropical Africa. Our results show that the δD values of the aquatic lipid biomarker *n*-C₁₇ alkane were not correlated with the δD values of lake water. Carbon isotope measurements indicate that the *n*-C₁₇ alkane was derived from multiple source organisms that used different hydrogen pools for biosynthesis. We demonstrate that the δD values of the *n*-C₂₉ alkane were correlated with the δD values of surface water (i.e., river water and groundwater), which, on large spatial scales, reflect the isotopic composition of mean annual precipitation. Such a relationship has been observed at higher latitudes, supporting the robustness of the leaf-wax lipid δD proxy on a hemispheric spatial scale. In contrast, the δD values of the *n*-C₃₁ alkane did not show such a relationship but instead were correlated with the evaporative lake water δD values. This result suggests distinct water sources for both leaf-wax lipids, most likely originating from two different groups of plants. These new findings have important implications for the interpretation of long-chain *n*-alkane δD records from ancient lake sediments. In particular, a robust interpretation of palaeohydrological data requires knowledge of the vegetation in the catchment area as different plants may utilise different water sources. Our results also suggest that the combination of carbon and hydrogen isotopes does help to differentiate between the metabolic pathway and/or growth form of organisms and therefore, the source of hydrogen used during lipid biosynthesis.

© 2011 Elsevier Ltd. All rights reserved.

* Corresponding author. Address: DFG-Leibniz Center for Surface Process and Climate Studies, Institut für Erd- und Umweltwissenschaften, Universität Potsdam, Karl-Liebknecht-Str. 24, Haus 27, 14476 Potsdam-Golm, Germany. Tel.: +49 331 977 5837; fax: +49 331 977 5700.

E-mail address: yannickgarcin@yahoo.fr (Y. Garcin).

1. INTRODUCTION

The tropics play a key role in global climate, as they are the main source of heat and water vapour for Earth's atmospheric convection processes. These processes drive climatic variability on a global scale, such as the El Niño–Southern Oscillation phenomenon (ENSO) (Cane, 2005). In tropical Africa, the hydrological cycle is the dominant component of the climate system, and it affects ecology, the economy, and the well being of humans (Birkett et al., 1999; Nicholson, 2001; de Wit and Stankiewicz, 2006). Temperature variability is only of secondary importance as the diurnal range is generally higher than seasonal and interannual variability.

To better assess present-day climate variability and future changes of the climate system, it is important to understand the forcings and characteristics of past climatic changes that can be evaluated in a variety of geological archives. Such climate proxies include the stable isotopes of water (D/H and $^{18}O/^{16}O$ expressed as δD and $\delta^{18}O$, respectively) that have been extensively used to understand the present-day and past hydrological cycle (e.g., Craig, 1961; Dansgaard, 1964; Rozanski et al., 1993). The interest in refining isotopic tools for the reconstruction of past climatic changes results from the apparent link between the amount of rainfall (and/or the temperature) and the spatial patterns of δD and $\delta^{18}O$ measured under present-day climatic conditions (e.g., Craig, 1961; Dansgaard, 1964; Rozanski et al., 1993; Jouzel et al., 2000). Because water is the source of hydrogen and oxygen in the metabolism of plants and animals and is an important constituent in certain minerals, a large number of climate proxies devoted to the analysis of δD and $\delta^{18}O$ from plant remains, tree rings, bones, shells, speleothems, and clays have been developed (e.g., Kohn et al., 1996; McDermott, 2004; Leng, 2006; Mulch et al., 2006; Kahmen et al., 2011a). However, a quantitative reconstruction of past climatic changes from isotopic proxy records requires a good mechanistic understanding of the fractionation processes of the stable isotopes during biosynthesis as well as mineral precipitation. Therefore, the driving forces of these processes need to be appropriately calibrated to use these approaches with a high level of confidence.

Interest in compound-specific hydrogen isotope ratio analysis as a continental palaeohydrological proxy has emerged during the past decade and is increasingly used (e.g., Sessions et al., 1999; Andersen et al., 2001; Sauer et al., 2001; Huang et al., 2002, 2004; Sachse et al., 2004, 2006; Hou et al., 2008), reflecting the need to provide new high fidelity palaeohydrological records. Studies to discriminate the physiological factors and environmental processes involved in lipid δD values have been performed on several marine and terrestrial ecosystems (e.g., Sessions et al., 1999; Sauer et al., 2001; Chikaraishi and Naraoka, 2003; Sachse et al., 2006; Hou et al., 2007; Feakins and Sessions, 2010; Polissar and Freeman, 2010; McInerney et al., 2011; Sachs and Schwab, 2011). These studies have ultimately resulted in the establishment of regional calibrations relating lipid δD values with lake and precipitation δD values (e.g.,

Huang et al., 2002, 2004; Sachse et al., 2004; Hou et al., 2008; Xia et al., 2008).

To date, calibration studies for sedimentary lipid δD have only been available for mid- to high-latitude environments (Sauer et al., 2001; Huang et al., 2004; Sachse et al., 2004; Hou et al., 2008; Mügler et al., 2008; Xia et al., 2008; Aichner et al., 2010b). A recent calibration study of sedimentary *n*-alkane δD included several sites from tropical South America (Polissar and Freeman, 2010), although most of these sites were from high-elevation areas (>3500 m), and no low-elevation data have been obtained in a systematic way. However, a calibration focusing specifically on the tropical realm, which occupies half of the Earth's surface, does not yet exist. The need for such a calibration is important because lipid biomarker δD values are increasingly used to reconstruct past changes in tropical African hydrology (e.g., Schefuß et al., 2005; Barker et al., 2007; Tierney et al., 2008, 2011; Russell et al., 2009; Niedermeyer et al., 2010). Due to our limited understanding of the factors controlling lipid δD values of aquatic and terrestrial photosynthesising organisms in tropical ecosystems, which are highly diverse and often distinct in comparison to the extra-tropical ecosystems studied thus far, these reconstructions are presently only qualitative at best.

Among the large group of lipids produced by photosynthesising organisms, *n*-alkanes are well suited for palaeoproxy development (Sachse et al., 2004). These compounds are abundant in lacustrine sediments and do not require large samples for measuring their δD values (~1 g of dry sediment needed with an organic carbon content of 5%). Therefore, the δD values of *n*-alkanes can be measured routinely in different continental environments. The *n*-alkanes are relatively resistant to microbial breakdown, and they remain highly stable, at least at lower temperatures, because their hydrogen atoms are carbon-bound and therefore, non-exchangeable (Schimmelmann et al., 1999). Moreover, *n*-alkanes with a different number of carbon atoms are often associated with different biological sources (e.g., algae, aquatic, and terrestrial plants) (Eglinton and Hamilton, 1967; Gelpi et al., 1970; Cranwell et al., 1987; Ficken et al., 2000; Meyers, 2003).

Here, we identify the main environmental processes that control the hydrogen isotopic composition of sedimentary *n*-alkanes and develop a solid framework for the quantitative application of compound-specific hydrogen isotopes in tropical Africa. For this purpose, a 8°-long latitudinal transect of lake basins across Cameroon was chosen because it encompasses a wide range of contrasting climates and vegetation classes that are representative of the entire tropical African realm. We measured the δD values of sedimentary *n*-alkanes ($\delta D_{n\text{-alkane}}$) along extraordinarily steep climate and vegetation gradients as well as the δD values of a wide range of water sources, including lake water, precipitation, river water, groundwater, and plant-xylem water. Our approach allows us to identify the potential source organisms and the environmental water pools feeding into *n*-alkane biosynthesis. Finally, our data validate the use of sedimentary lipid δD as a robust proxy for surface water δD and possibly for evaporation in tropical Africa.

2. STUDY SITE

From the southwest to the north, Cameroon contains the main physiographic settings, climates, and vegetation classes of the African continent (Olivry, 1986) and thus constitutes an ideal natural setting to evaluate the relationship between lacustrine sedimentary lipid δD and source water δD (Fig. 1).

Southern Cameroon (excluding the Atlantic Coast) comprises a relatively flat plateau landscape gently sloping towards the east, with elevations of 700–800 m asl and 400 m asl in the western and eastern sector, respectively. The climate is humid with two precipitation maxima following the equatorial high-sun seasons, during the spring

and autumn equinoxes. The average annual temperature and precipitation are 24 °C and 1500 mm, respectively (Sudchel, 1987). The vegetation is of the Lower Guinea and Congolia type (White, 1983), including moist evergreen and semi-evergreen rainforests and a drier rainforest in which each of the common largest tree species are more deciduous than in the evergreen forest (Letouzey, 1968, 1985; Tchouto Mbatchou, 2004).

The Atlantic Coast has a hot and humid climate. The mean annual temperature is 26 °C, and the annual precipitation is ~3000–4000 mm, with high relative humidity (~85%) throughout the year and without a marked dry season. On the exposed slopes of Mount Cameroon (rising up to 4040 m asl), precipitation is almost continuous

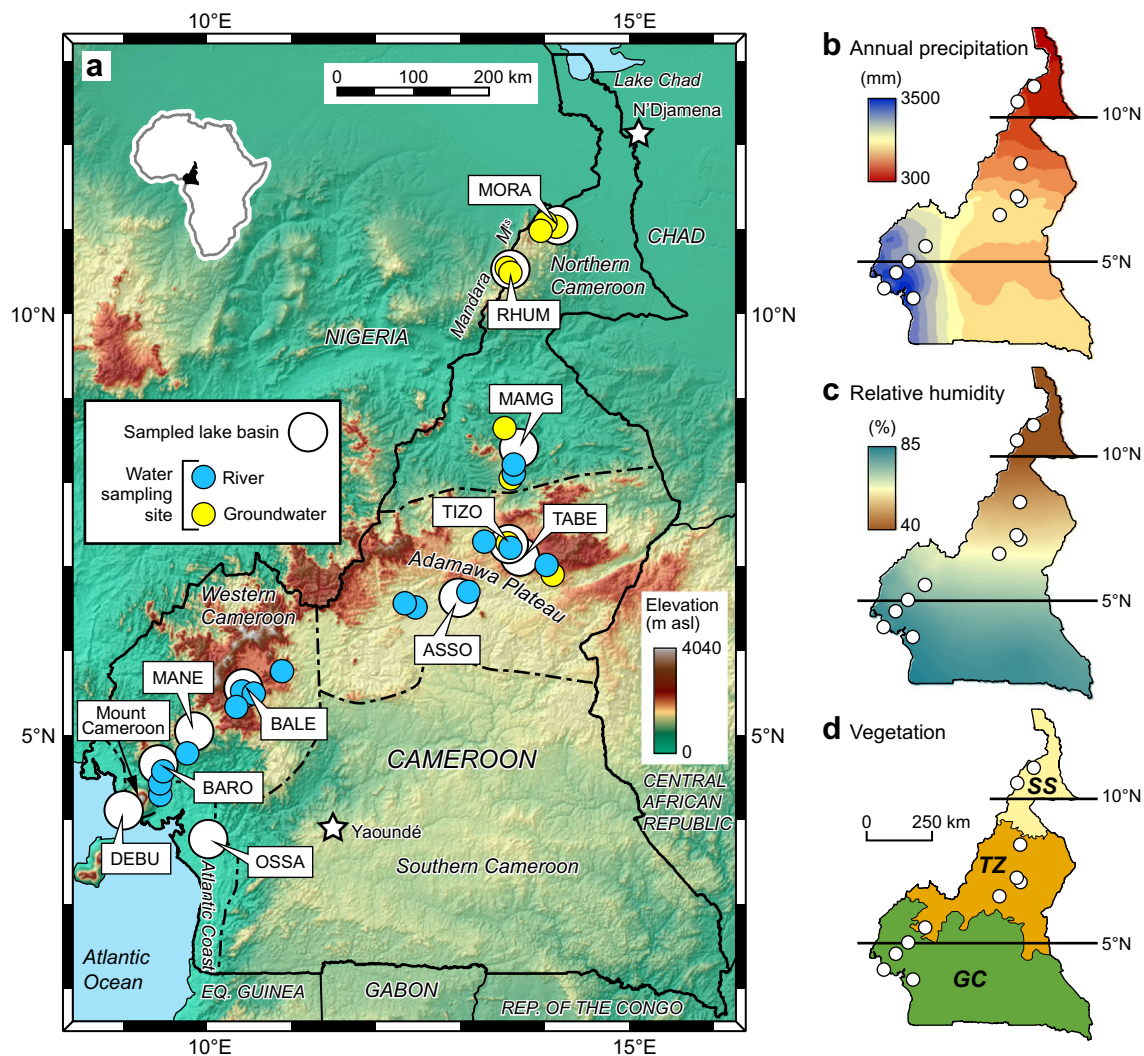


Fig. 1. Modern lake transect in Cameroon. (a) Location of the 11 investigated lake basins overlain on a Shuttle Radar Topography Mission digital elevation model. Also shown are additional sites sampled for environmental water isotope analysis (rivers and groundwaters). Dashed lines bound the natural regions as described in the main text. (b) Mean annual precipitation, CRU CL 2. dataset (New et al., 2002). (c) Relative humidity, CRU CL 2. dataset (New et al., 2002). (d) Simplified vegetation map, adapted from the TREES project (Mayaux et al., 1999), showing the main phytogeographical regions (White, 1983): GC = Lower Guinea and Congolia rainforest; TZ = transition zone, including tree savanna and woodland; SS = Sudano-Sahelian shrub savanna. Sampled lake basins are overlaid on climatology and vegetation maps.

throughout the year and can reach 12000 mm yr⁻¹ (Lefèvre, 1967; Fontes and Olivry, 1976). Evergreen rainforest and mangrove swamps characterise the coastal vegetation (Letouzey, 1968, 1985).

Western Cameroon is mountainous, with elevations ranging from 700 to 2400 m asl. This region is characterised by a cooler mean annual temperature of ~18 °C. The mean annual precipitation is high (~2000 mm) and occurs from March to November. In this highly populated area, natural vegetation (e.g., evergreen highland forest) has locally been strongly altered by human activities (Letouzey, 1968, 1985).

The central area of Cameroon (Adamawa Plateau) constitutes a region with elevations reaching ~1500 m asl. The mean annual temperature is 22 °C, and the mean annual precipitation is ~1500 mm. The rainy season is limited to 7 months (April–October). The vegetation belongs to the Sudano-Guinean type, which is transitional between forest in the south and savanna in the north (White, 1983).

Northern Cameroon is mostly a lowland area (excluding the Mandara Mountains), with a mean elevation of 200–400 m asl. The mean annual temperature is 27 °C, with large diurnal temperature variations of ~14 °C (Suchel, 1987). The mean annual precipitation is 700 mm, with a short 5-month rainy season (May–September). The relative humidity is low (~50%). The transitional vegetation to the south grades rapidly towards the north into a vegetation typical of the Sudano-Sahelian domain, being composed of steppe with thorny shrubs, bushes, and grasses (White, 1983). In the far north, the dry savanna/steppe is progressively replaced by low-elevation marshland (at ~290 m asl) surrounding Lake Chad (Letouzey, 1968, 1985).

3. MATERIALS AND METHODS

3.1. Sampling

During November 2009, we sampled 11 lake basins distributed along a SW–NE latitudinal transect across Cameroon, from 3.7 to 11°N (Fig. 1; Tables 1 and 2). For each site, samples were collected within 1 or 2 days. We focused on crater lakes because their small catchment areas lead to relatively fast transportation (via streams, sheet wash erosion, and wind transport of canopy leaves) of local terrestrial compounds (e.g., leaf waxes) to the deep lake. Moreover, the steep inner slopes of the crater lakes generally protect them from human activities, such as deforestation and subsequent soil erosion. Six of the studied lake basins were crater lakes, the remainder comprising two shallow lakes, one quarry lake, and two artificial reservoirs. All lakes were freshwater lakes (Table 2).

3.1.1. Water

To constrain the isotopic composition of the water sources used by terrestrial plants, we collected plant stem samples for xylem-water extraction, river water, and groundwater (from wells) in the vicinity of the studied sites as well as precipitation from localised and sporadic rainfall

events occurring in Cameroon during May, October, and November 2009. Stems were cut from several local tree species (five species were sampled per site). After the phloem was removed, the stems were immediately enclosed in screw cap polypropylene vials and tightly sealed with electrical tape. The xylem samples were kept frozen in the laboratory until analysis. The river, groundwater, and precipitation samples were collected in screw cap polypropylene vials, which were tightly sealed with electrical tape, and stored at 4 °C until analysis. The lake water samples were collected at various depths (up to 40-m deep) using an electric submersible pump (model QGDa series) connected to a custom filtration unit (MPI–BGC Jena) with a 50-m-long PVC flexible pipe as well as two stainless steel prefilters of 50 µm and 10 µm and a removable glass fibre filter (1-µm pore size). The lake water temperature, conductivity, and pH were measured with a multiprobe (YSI 6600 profiler, Yellow Springs, Ohio, USA), ensuring the comparability of the lake characteristics (Table 2).

3.1.2. Lake sediment

Lake sediment was collected using a gravity corer (HTH-Teknik, Luleå, Sweden) operated from an inflatable raft. The uppermost sediment, corresponding to an uncompacted soupy layer (upper 1–4 cm) and covering approximately the last few years of sedimentation, was collected up to four times, usually in the deepest and central part of the lake, as determined by echo sounding. For the two deepest lakes (>100 m; i.e., Barombi Mbo and Manengouba), sediments were collected on shallower plateau areas. The sediment samples were freeze-dried, coarse vegetation debris was removed using tweezers, and finally, the samples were ground.

3.1.3. Lake particulate organic matter

Lake particulate organic matter (POM) was collected at a depth of 1 m using an electric submersible pump (model QGDa series) connected to a custom filtration unit (MPI–BGC Jena). Glass fibre filters (10 µm > Ø > 1 µm) were dried in situ.

3.1.4. Soil

To determine the composition of *n*-alkanes produced by terrestrial plants in the lake catchments, several topsoil samples (0–5-cm deep), which integrate the *n*-alkane composition from the above vegetation in time and space, were collected using a hand-operated soil sampler (Eijkelkamp, Giesbeek, The Netherlands) at six selected catchments along the transect. Before analysis, the soil samples were freeze-dried and subsequently sieved using a mesh size of 600 µm to remove roots and other coarse materials. Furthermore, the estimate of the wood/grass ratio, which is an indicator for the composition of local vegetation, was determined in situ for each site.

3.2. Analyses

3.2.1. Water δD and $\delta^{18}\text{O}$ values

Water isotope data on all water samples were measured at MPI–BGC Jena. The xylem water was extracted from

Table 1

Location and basic geographical, morphometrical, and meteorological data of the sampled lake basins.

Site code	Lake	Type ^a	Lat. (°N) ^b	Long. (°E) ^b	Elevation (m asl) ^b	Max. depth (m) ^c	Lake area (ha) ^d	Catchment area (ha) ^d	MAT (°C) ^e	MAP (mm) ^f
MORA	Mora	TR	11.0547	14.1457	438	1.5	0.1	7	27.2	540
RHUM	Rhumsiki	PR	10.5082	13.5838	1028	3	1.3	140	22.7	970
MAMG	Mamguiewa	QL	8.3909	13.7089	322	5	0.6	2	26.3	1560
TIZO	Tizong	CL	7.2533	13.5769	1155	45	7	17	21.9	1450
TABE	Tabéré	CL	7.1307	13.6940	1161	62	10	46	21.7	1450
ASSO	Assom	SL	6.6245	12.9816	896	3	141	4500	23.0	1740
BALE	Baleng	CL	5.5503	10.4211	1376	52	11	18	20.5	1850
MANE	Manengouba F. ^g	CL	5.0364	9.8284	1911	165	35	105	16.0	2700
BARO	Barombi Mbo	CL	4.6544	9.4086	304	110	410	800	24.9	2550
DEBU	Debundscha	CL	4.1034	8.9805	70	16	7	5	25.7	11700
OSSA	Ossa	SL	3.7686	10.0049	17	6	3700	16500	26.3	2900

^a SL = shallow lake; CL = crater lake; QL = quarry lake; PR = permanent reservoir; TR = temporary reservoir.^b Determined in situ using a handheld GPS.^c Maximum water depth determined in situ using an echosounder.^d Data from Kling (1988) complemented by estimates from Google Earth®.^e MAT = mean annual air temperature; estimated using the WorldClim 2.5' gridded dataset (Hijmans et al., 2005).^f MAP = mean annual precipitation; estimated using local raingauge data (CIEH, 1990).^g Female lake; other name: Mwanenguba.

Table 2

Limnological and vegetation data of the sampled lake basins as determined in situ. Sites are presented from south to north reading from bottom to top, respectively.

Site code	Lake	Vegetation				
		Coring depth (m) ^a	Temperature (°C) ^b	pH ^b	Conductivity ($\mu\text{S cm}^{-1}$) ^b	Zone ^c
MORA	1.5	31	8.8	116		SS 10/90
RHUM	2.8	23.5	7.8	145		SS 10/90
MAMG	5	25.5	8	155		TZ 40/60
TIZO	43	24.5	8.5	175		TZ 50/50
TABE	60	23.5	7.5	89		TZ 50/50
ASSO	3	28	6.5	97		TZ 40/60
BALE	50	26	7.1	126		TZ 50/50
MANE	40	20.5	7	32		TZ 30/70
BARO	65	29	7.3	40		GC 80/20
DEBU	16	29	7	38		GC 95/5
OSSA	6	29	6	22		GC 80/20

^a Determined using an echosounder.^b Measurement at lake surface.^c Phytogeographical zones: GC = Lower Guinea and Congolia; TZ = transition zone; SS = Sudano-Sahelian.

stem samples using cryogenic vacuum distillation following the method described by West et al. (2006). The xylem water isotope ratios were measured by online high temperature reduction in the modified carbon reactor of a high-temperature elemental analyser (TC/EA) coupled to an isotope ratio mass spectrometer (Delta^{plus}XL, Finnigan MAT Bremen, Germany) (Gehre et al., 2004). The average standard deviation was 1.3‰ for δD and 0.1‰ for δ¹⁸O ($n = 60$). The lake water, river water, groundwater, and precipitation samples were measured using a Cavity Ring-Down Spectrometry (CRDS) analyser (L1102-i, Picarro, Sunnyvale, USA) following the method described by Brand et al. (2009). The average standard deviation was 0.5‰ for δD and 0.06‰ for δ¹⁸O ($n = 93$).

3.2.2. Preparation of sediment, filter, and soil samples, lipid biomarker identification and quantification

The sediment, filter, and soil samples were extracted using an accelerated solvent extractor (ASE350, Dionex Corp., Sunnyvale, USA) with a dichloromethane/methanol mixture (9:1) at 100 °C and 1500 psi for three 10-min cycles at the University of Potsdam. Depending on the amount of organic carbon in the sample, 2–15 g of sediment and/or soil sample was used for extraction. The total extract was separated using solid phase extraction (SPE) on silica gel. Glass columns (6 ml; Macherey-Nagel, Düren, Germany) were filled with 1.5 g of silica gel (0.040–0.063 mesh; Alfa Aesar, Ward Hill, USA) previously dried at 60 °C. The n-alkanes were eluted with hexane (10 ml). Due to the presence

of an abundant unresolved complex mixture (UCM) in most of the POM (filter) samples, their hydrocarbon fraction was further purified using a Linde 5A molecular sieve following the method described by Grice et al. (2008). All other samples did not require molecular sieve purification since their chromatograms showed baseline-separated peaks. The compounds were identified and quantified using gas chromatography with a coupled flame ionisation detection and mass-selective detector (GC-FID/MSD Agilent 7890A GC, 5975C MSD, Agilent Technologies, Palo Alto, USA) at the University of Potsdam. The GC-FID/MSD was equipped with an HP5-MS capillary column (30 m × 0.25 mm, 0.25- μm film thickness). Helium was used as the carrier gas, and the temperature of the GC oven was programmed to an initial temperature of 70 °C (held for 2 min), a heating rate of 12 °C min⁻¹, and a final temperature of 320 °C (held for 21 min). The PTV injector was held at a split ratio of 5:1 at an initial temperature of 70 °C. With injection, the injector was heated to 300 °C at a programmed rate of 720 °C min⁻¹ and held at this temperature for 2.5 min. For quantification, the FID-peak areas of the *n*-alkanes were compared with those from an external *n*-alkane standard mixture as well as those from two internal standards: 5 α -androstane (10 μg) and methyl behenate (100 μg), added before and after the extraction phase, respectively. The *n*-alkane concentrations in the lake sediment, lake POM, and soil samples are given in the relative abundance of total *n*-alkanes (calculated to a sum of 1). The *n*-alkane concentrations were also calculated relative to the total organic carbon ($\mu\text{g g}^{-1}$ TOC) for the lake sediment samples.

3.2.3. Bulk total organic carbon analysis on lake sediments

Determinations of the TOC from the sediment samples were carried out on decalcified samples. Approximately 5–10 mg of sediment was weighed in Ag capsules, treated with 25% HCl, heated overnight at 90 °C, and wrapped up in the Ag capsules. The Ag capsules were finally wrapped up in Sn capsules. The carbon content was measured at the University of Potsdam using a vario EL elemental analyser (Elementar Analysensysteme GmbH, Hanau, Germany) equipped with a thermal conductivity detector. The average standard deviation was 1%.

3.2.4. δD and $\delta^{13}\text{C}$ values of sedimentary *n*-alkanes

The δD values were determined on the *n*-alkane fraction of lake sediment samples only, using a coupled gas chromatography-isotope ratio mass spectrometry system (GC-IRMS) at MPI-BGC Jena. The *n*-alkane fraction dissolved in hexane was injected (1 μl) into an HP5890 GC (Agilent Technologies, Palo Alto, USA) equipped with a BP1 column (60 m × 0.32 mm, 0.5- μm film thickness, SGE Analytical Science, Ringwood, Australia). The injector was operated at 280 °C in splitless mode. The oven was maintained for 1 min at 60 °C, heated at 10 °C min⁻¹ to 300 °C, and held there for 30 min, after which it was ramped to 340 °C at 20 °C min⁻¹ and held at this final temperature for 3 min. The column flow was constant at 2 ml min⁻¹. To monitor the possible coelution of *n*-alkanes with other compounds, part of the column effluent was transferred to an ion trap

mass spectrometer (GCQ ThermoElectron, San José, USA). The remainder of the split went to an isotope mass spectrometer via quantitative conversion to H₂ in a high-temperature oven operated at 1425 °C (Burgoyne and Hayes, 1998; Hilkert et al., 1999). Compound-specific δD values were obtained using a Delta^{plus}XL IRMS (Finnigan MAT, Bremen, Germany). The results are reported in conventional delta notation (i.e., δD values) in permil (‰) units. Each sample was analysed at least in triplicate. When the *n*-alkane concentration was too low, the hydrocarbon fraction was further concentrated and injected manually into the GC. H₂ gas of a known isotopic composition was used as a working reference standard. The δD values were corrected to the Vienna Standard Mean Ocean Water (VSMOW) scale using a standard mixture of *n*-C₁₄ to *n*-C₃₃ alkanes. The values in the standard mixture were calibrated against international reference substances (NBS-22; IAEA-OH22) using the offline high temperature pyrolysis technique (TC/EA; Gehre et al., 2004). Because the concentration of long-chain and short-chain *n*-alkanes was highly variable within a sample (except for samples OSSA and ASSO), two separate sample runs with appropriate dilutions were conducted to ensure that the peak area of the compounds of interest was similar to the peak area of the compounds in the standard mixture. The accuracy was evaluated by routine measurement of the standard mixture after every six injections (two samples). If necessary, a drift correction was applied. To ensure stable ion-source conditions during measurement, the H₃⁺ factor (Hilkert et al., 1999) was determined at least once a day and was constant over the one-week measurement period at 6.4 (SD = 0.2). The achieved precision was expressed as the average standard deviation for all peaks having a clean baseline separation: 5‰ for the samples ($n = 390$, 75 runs with 1–15 peaks, depending on sample) and of 4‰ for the standard mixtures ($n = 612$, 36 runs with 17 peaks each).

The $\delta^{13}\text{C}$ values were determined on the same fraction previously measured for δD . The instrumental setup (GC-IRMS), the GC column, and the temperature programme used were identical to the δD measurements. The oxidation oven was operated at 960 °C. The results are reported in conventional delta notation (i.e., $\delta^{13}\text{C}$ values) in permil (‰) units. CO₂ gas of a known isotopic composition was used as a working reference standard. The $\delta^{13}\text{C}$ values were corrected to the Vienna Standard Pee Dee Belemnite (VPDB) scale using the same *n*-alkane mixture as for hydrogen, with predetermined TC/EA $\delta^{13}\text{C}$ values. The achieved precision was 0.6‰ for the samples ($n = 120$, 60 runs with 1–3 peaks, depending on the sample) and 0.5‰ for the standard mixtures ($n = 330$, 35 runs with 9 peaks each).

Hydrogen and carbon isotopes are reported only for *n*-C₁₇, *n*-C₂₉, and *n*-C₃₁ alkanes (i.e., $\delta D_{n\text{-}C17}$, $\delta D_{n\text{-}C29}$, $\delta D_{n\text{-}C31}$ and $\delta^{13}\text{C}_{n\text{-}C17}$, $\delta^{13}\text{C}_{n\text{-}C29}$, $\delta^{13}\text{C}_{n\text{-}C31}$, respectively) because these compounds were present in sufficient amounts for isotopic analysis (for most sites) and were characterised by baseline-separated peaks. Most of the other *n*-alkane homologues were discarded because they either interfered with other coeluting compounds or were only present in minor amounts, thus preventing high-precision isotopic analysis. A few other *n*-alkane homologues, which showed

clean baseline-separated peaks and sufficient amounts for isotopic analysis, are not discussed here as they were only present in a small number of samples.

We reported isotopic fractionations (or offsets) between two measured substances (in permil notation), δD_a and δD_b , as enrichment factors ($\varepsilon_{a/b}$) defined as:

$$\varepsilon_{a/b} = \alpha_{a/b} - 1 = \frac{\delta D_a + 1}{\delta D_b + 1} - 1 \quad (1)$$

4. RESULTS AND DISCUSSION

4.1. δD values of surface water

To identify the hydrogen sources of sedimentary lipids, it is essential to compare lipids with a robust dataset of the isotopic composition of their potential water sources, such as precipitation and lake water. The isotope data from the Global Network of Isotopes in Precipitation (GNIP) on the African continent are scarce (IAEA/WMO, 2006). Only one station is available near the study area: N'Djamena (294 m asl, 12°N), in Chad, located along the border with Cameroon (Fig. 1). Hence, using interpolated datasets (e.g., Bowen and Revenaugh, 2003) for the estimation of mean annual δD values of precipitation does not result in reliable estimates.

As no mean annual precipitation δD values are available for any of the studied sites, we established a dataset of flowing surface waters (e.g., small rivers and shallow groundwaters) for comparison. Although the isotopic composition of rivers and shallow groundwaters do not systematically mirror the isotopic composition of local precipitation due to variability in residence time, catchment size, and evaporative processes, such data are considered valuable indicators of the isotopic composition of precipitation in regions where long-term precipitation δD values are missing (Kendall and Coplen, 2001; Poage and Chamberlain, 2001; Lachniet and Patterson, 2002; Rowley and Garzzone, 2007; Hoke et al., 2009; Levin et al., 2009).

Tritium (3H) measurements of various shallow groundwaters from both southern and northern Cameroon have indicated short residence times (<30 yr) of water, supporting the use of surface groundwaters to infer present-day mean precipitation δD values (Ketchemen et al., 1993; Njitchoua et al., 1995; Ako et al., 2009; Fantong et al., 2010). Moreover, the hydrogen and oxygen isotopic composition of shallow groundwaters across Cameroon mostly plot close to or along the Global Meteoric Water Line (GMWL; Craig, 1961), indicating that they are derived from meteoric water (Ketchemen et al., 1993; Njitchoua et al., 1995; Tanyileke et al., 1996; Ako et al., 2009; Fantong et al., 2010). In northern Cameroon, it was further observed that the isotopic composition of groundwaters is seasonally stable, suggesting that groundwater recharge occurs at a decadal scale in this region (Ketchemen et al., 1993).

From our water dataset, which mostly consists of isotopic values for local rivers (with a limited catchment area <2000 km²), shallow groundwaters, local precipitation, and lake-bottom waters for two coastal sites, we derived a

mean surface water δD value (δD_{SW}) for each of the sampled lake basins (raw data and calculation methods are available in [Electronic Annex EA-1 and EA-2](#)). The δD_{SW} values ranged from -38.8 to -8.4‰ (Table 3, Figs. 2 and 3c). Near the Atlantic coast, the δD_{SW} values from sites OSSA and DEBU were the most D-enriched, with values of -12.6‰ and -8.4‰ , respectively. Conversely, the northernmost site, MORA, had a relatively D-depleted δD_{SW} value of -27.6‰ . This value falls within the range of variation of precipitation δD recorded from the nearby N'Djamena GNIP station (located ~ 150 km NE of MORA), where a value of $-21.5 \pm 10\text{‰}$ was obtained during 11 years of measurements between 1964 and 1995 (IAEA/WMO, 2006).

To test whether our surface water δD values were representative for precipitation δD values (δD_{PW}), we compared the local surface water line (LSWL) to the GMWL. As shown in Fig. 2, the Cameroon LSWL, defined as $\delta D = 8.3 \times \delta^{18}\text{O} + 14.2$, was similar to the GMWL of $\delta D = 8 \times \delta^{18}\text{O} + 10$ (Craig, 1961). Moreover, the sampled rainfall events ([Electronic Annex EA-3](#)) plotted along the LSWL further supported the use of δD_{SW} values as an estimation of δD_{PW} values (Fig. 2). However, the isotopic composition of the surface waters may have differed locally from that of precipitation, even if the data points lay on the GMWL. For example, if evaporation occurred at high relative humidity ($\sim 90\text{--}100\%$), the isotopic values of the sampled surface waters would evolve along a line that is nearly parallel to the GMWL (Gat and Gonfiantini, 1981), thus potentially altering the δD_{SW} values of the southernmost sites (i.e., OSSA, DEBU, and BARO), which are characterised by humid climates. For this reason, we do not seek to interpret our surface water data in terms of precipitation δD values *sensu stricto*.

To assess whether the actual plant available water tracked δD_{SW} , we also analysed plant xylem water δD values (δD_{XW}). Xylem water is thought to reflect the isotopic composition of precipitation (or groundwater), which is transported in the xylem without any isotopic alteration during uptake by the roots (Dawson and Ehleringer, 1991). However, due to soil evaporation, pools of water in the soil available to plants are sometimes isotopically distinct, with the topsoil water being more D-enriched than the deeper soil water (Barnes and Allison, 1988), altering the original isotopic composition of the precipitation. In Cameroon, the δD_{XW} and $\delta^{18}\text{O}_{XW}$ values (average per site) generally plotted along the LSWL (Fig. 2), although several of the xylem samples showed minor effects of evaporation, denoted by their position slightly below the LSWL (hydrogen and oxygen isotope data for all xylem waters are reported in the [Electronic Annex EA-4](#)). Because the δD_{XW} and δD_{SW} values covaried along the gradient (except for site MAMG; see Fig. 3c), we conclude that surface waters represented the plant water available for the lipid biosynthesis of terrestrial plants. The relatively large variability in the δD and $\delta^{18}\text{O}$ values for the xylem waters at one site reflected either differences in soil water pools used by local plants and/or differences in the timing of seasonal plant water uptake. At site MAMG, the 14‰ offset between the δD_{XW} and δD_{SW} values is possibly related to local variability in the depths of roots from the sampled plant species,

Table 3

Isotopic composition of environmental waters for each of the sampled lake basins. Sites are presented from south to north reading from bottom to top, respectively.

Site code	$\delta^{18}\text{O}_{\text{LK}}$ (‰)	SD	$\delta\text{D}_{\text{LK}}$ (‰)	SD	$\delta^{18}\text{O}_{\text{SW}}^{\text{a}}$ (‰)	SD	$\delta\text{D}_{\text{SW}}^{\text{a}}$ (‰)	SD	$\delta^{18}\text{O}_{\text{XW}}^{\text{b}}$ (‰)	SD	$\delta\text{D}_{\text{XW}}^{\text{b}}$ (‰)	SD
MORA	2.59	0.05	+12.4	0.6	-4.49	0.49	-27.6	3.4	-3.26	0.64	-27.3	4.7
RHUM	-0.59	0.05	-0.7	0.8	-4.31	0.07	-26.0	0.8	-4.28	1.29	-33.8	7.3
MAMG	1.91	0.03	5.6	0.6	-3.57	0.79	-17.9	4.1	-5.03	1.19	-32.3	6.2
TIZO	4.64	0.03	+22.8	0.0	-3.67	0.58	-15.6	3.7	-3.18	2.26	-19.8	9.9
TABE	1.15	0.05	11.4	0.5	-3.67	0.58	-15.6	3.7	-2.54	0.74	-15.2	9.1
ASSO	-1.19	0.06	-4.7	0.8	-3.54	0.33	-14.9	2.4	-1.73	0.51	-11.4	4.1
BALE	0.25	0.02	0.6	0.6	-4.28	0.44	-19.8	6.0	-2.62	1.40	-19.3	9.9
MANE	-1.03	0.04	-6.1	0.3	-6.13	n.a.	-38.8	n.a.	-5.21	1.05	-36.1	6.6
BARO	-0.28	0.05	2.2	0.0	-3.67	0.47	-15.8	2.9	-3.59	0.42	-20.7	3.0
DEBU	-2.40	0.02	-8.7	0.7	-2.44	0.04	-8.4	0.1	n.a.	n.a.	n.a.	n.a.
OSSA	-2.92	0.02	-11.9	0.7	-2.96	0.07	-12.6	0.3	n.a.	n.a.	n.a.	n.a.

n.a. = not available/not determined.

SD = standard deviation.

LK = lake water; SW = surface water; XW = xylem water.

^a Data derived from averaging local surface waters.

^b Data derived from averaging xylem waters.

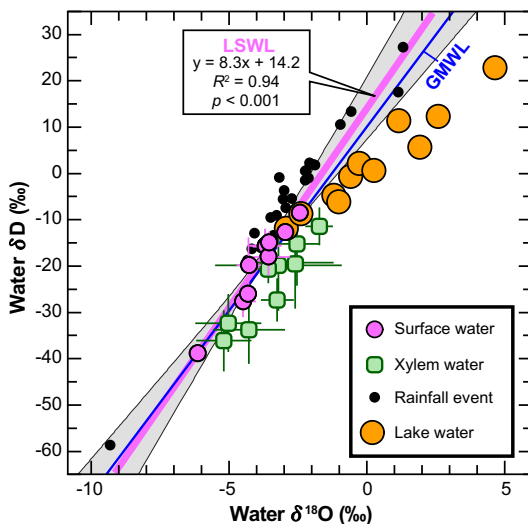


Fig. 2. Determination of source-water hydrogen and oxygen isotope ratios. δD and $\delta^{18}\text{O}$ values of surface water, xylem water, and lake water for each of the sampled lake basins in Cameroon. Data from localised and sporadic rainfall events sampled during the fieldwork are also shown. The local surface water line (LSWL, purple thick line) is defined from the estimated mean surface water values. Black lines bounding the grey area represent the 95% confidence intervals of the regression line (LSWL). The GMWL (see main text) is plotted for reference (blue line). Most data closely follow the LSWL with the exception of the lake waters that are subject to large evaporation effects. (For interpretation of the references to colour in this figure legend, the reader is referred to the web version of this article.)

which may derive their waters from a deep (older?) D-depleted water pool.

4.2. δD values of lake water

The lake surface water δD values ($\delta\text{D}_{\text{LK}}$) ranged from -11.9 to +22.8‰ and were significantly different from

$\delta\text{D}_{\text{SW}}$ (Table 3). The lowest $\delta\text{D}_{\text{LK}}$ value was found at site OSSA (-11.9‰) along the wet Atlantic Coast region. Towards the drier regions of northern Cameroon, the $\delta\text{D}_{\text{LK}}$ values became progressively more D-enriched (Fig. 3c), following the general increase in local evaporation (Suchel, 1987). The $\delta\text{D}_{\text{LK}}$ value of the northernmost site (MORA) was +12.4‰. Interestingly, the highest $\delta\text{D}_{\text{LK}}$ value was found at site TIZO (+22.8‰) from the central Adamawa region (Fig. 1), where local hydrological conditions probably prevailed. On a δD vs. $\delta^{18}\text{O}$ diagram, the lake water isotopic data plotted below and to the right of the LSWL (Fig. 2). This deviation from the LSWL is due to kinetic effects associated with the evaporative loss of the lake waters (Dansgaard, 1964; Craig and Gordon, 1965).

Our measured $\delta\text{D}_{\text{LK}}$ values represent a single instant in time and do not provide information on possible seasonal variations. Seasonal changes of surface water δD values in tropical Africa are best documented at Lake Masoko (Tanzania, 9°S), a crater lake similar to many of our sampled lakes (i.e., with a small catchment area and without contributions by large streams or rivers). The standard deviation of δD values from Lake Masoko, which was monitored monthly for a 36-month measurement period, was only 3‰, suggesting that seasonal effects on its $\delta\text{D}_{\text{LK}}$ values were small or negligible (Delalande, 2008). Similarly, the monthly monitoring of the Babogaya crater lake (Ethiopia) showed no pronounced seasonal variations and no changes of isotopic composition of water with depth (Kebede et al., 2004; Lamb et al., 2004).

Most of our studied lakes in Cameroon were stratified, with a well-developed thermocline and a pronounced anoxic hypolimnia (Kling, 1988). However, the analysis of lake water from different depths showed little variability of δD values with depth: the standard deviations from the water profile δD values were all lower than 3‰ (Electronic Annex EA-5 and EA-6). This homogeneity in the isotopic composition of the sampled lakes may suggest that their

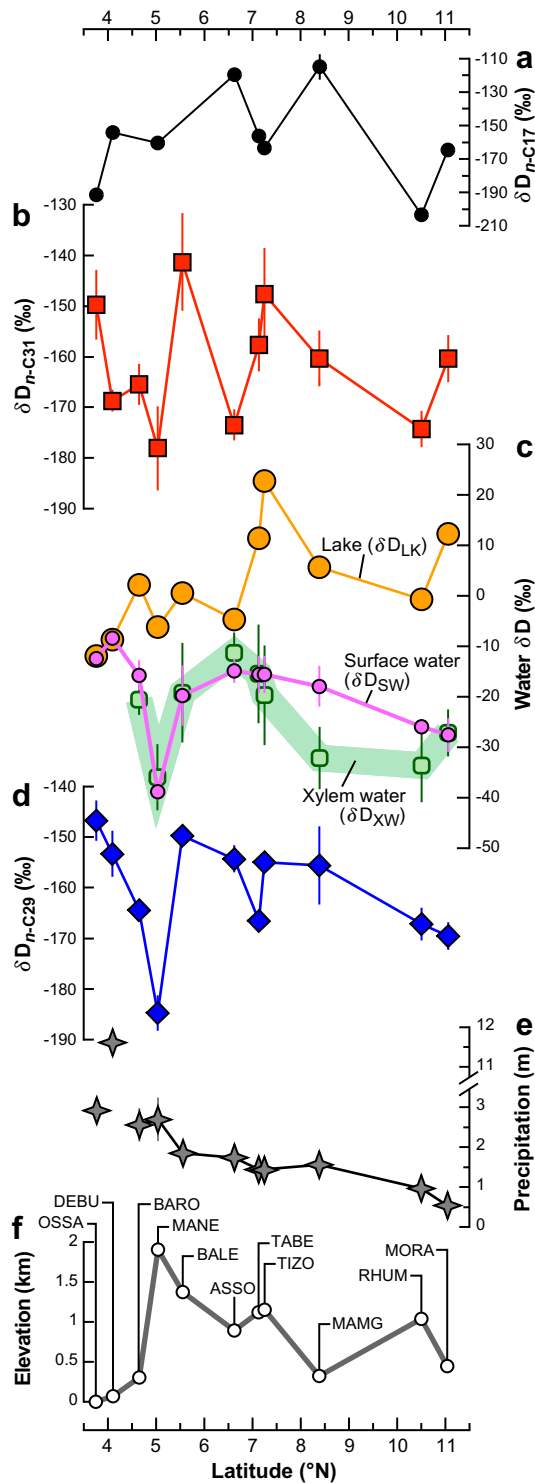


Fig. 3. Latitudinal changes in *n*-alkane δD , environmental water δD , precipitation, and elevation across the Cameroon transect. (a) $\delta D_{n\text{-C}17}$. (b) $\delta D_{n\text{-C}31}$. (c) δD_{LK} (orange line), δD_{SW} (purple line), and δD_{XW} (thick green line). (d) $\delta D_{n\text{-C}29}$. (e) Mean annual precipitation. (f) Elevation. (For interpretation of the references to colour in this figure legend, the reader is referred to the web version of this article.)

waters had relatively stable isotopic compositions on a seasonal timescale. Here, we hypothesised that the δD_{LK}

values for the studied lakes in Cameroon, at least from the wet southern region, were unaffected by large seasonal variations. However, the seasonal variability probably affected the shallower lakes to the drier north.

4.3. Sedimentary *n*-alkanes: composition and sources

The concentration of *n*-alkanes in the lake surface sediments along the Cameroon transect was highly variable (Fig. 4 and Electronic Annex EA-7). The lowest concentration of the dominant *n*-alkane was found in MORA ($n\text{-C}_{31} = \sim 60 \mu\text{g g}^{-1}$ TOC), whereas the highest concentration of the dominant *n*-alkane was found in MANE ($n\text{-C}_{29} = \sim 800 \mu\text{g g}^{-1}$ TOC). In general, the differences in the concentration of *n*-alkanes appear unrelated to latitude; however, they seem to be partly controlled by changes in elevation/temperature, as the higher elevation/cooler sites exhibited higher *n*-alkane concentrations (i.e., RHUM, BALE, and MANE), while the lower elevation/warmer sites had lower *n*-alkane concentrations (i.e., OSSA, DEBU, BARO, MAMG, and MORA; Fig. 3f and Fig. 4). The distribution of *n*-alkanes in the lake sediments ranged from $n\text{-C}_{13}$ to $n\text{-C}_{35}$, with a bimodal distribution reaching a maximum at $n\text{-C}_{17}$ and $n\text{-C}_{29}/n\text{-C}_{31}$, which is typical for sedimentary environments with dual sources of organic matter (Giger et al., 1980). All samples were characterised by an odd-over-even carbon number predominance, with carbon predominance index values (CPI, Fig. 4) between 2 and 11.6. The dominant *n*-alkanes in almost all lake sediments were the long-chain $n\text{-C}_{25}$ to $n\text{-C}_{33}$ homologues, represented by high average chain length values (ACL, Fig. 4) varying between 19.3 and 28.8. These distribution patterns are characteristic of *n*-alkanes mainly derived from the epicuticular leaf wax of terrestrial vascular plants (Eglinton and Hamilton, 1967). Long-chain $n\text{-C}_{25}$ to $n\text{-C}_{33}$ alkanes usually exhibited a clear bell-shaped distribution, which is commonly found in savanna tree, shrub, and herb species from tropical Africa (including both C₃ and C₄ photosynthetic pathways) (Rommerskirchen et al., 2006; Vogts et al., 2009). In BALE, the *n*-alkane distribution showed a narrower pattern with abundant $n\text{-C}_{29}$ and $n\text{-C}_{31}$ alkanes, which is analogous to the distribution patterns of rainforest plant species from tropical Africa (i.e., lianas, trees, and shrubs) (Vogts et al., 2009).

The short-chain $n\text{-C}_{17}$ alkane, likely derived from aquatic algae and bacteria (Han and Calvin, 1969; Gelpi et al., 1970; Cranwell et al., 1987; Meyers, 2003; Kristen et al., 2010), dominated the *n*-alkane composition in sediments from MAMG and ASSO, with concentrations of $\sim 750 \mu\text{g g}^{-1}$ TOC and $\sim 130 \mu\text{g g}^{-1}$ TOC, respectively. In OSSA, the $n\text{-C}_{21}$ alkane, likely derived from floating and/or submerged plants (Ficken et al., 2000), dominated with a concentration of $\sim 140 \mu\text{g g}^{-1}$ TOC.

To better constrain the sources of sedimentary *n*-alkanes, we compared the distribution patterns of *n*-alkanes from topsoil, lake water POM, and lake-sediment samples along the natural transect (Fig. 5 and Electronic Annex EA-8). The topsoil samples, which integrate the *n*-alkane composition of the local vegetation for representative sites, showed a unimodal distribution pattern typical of

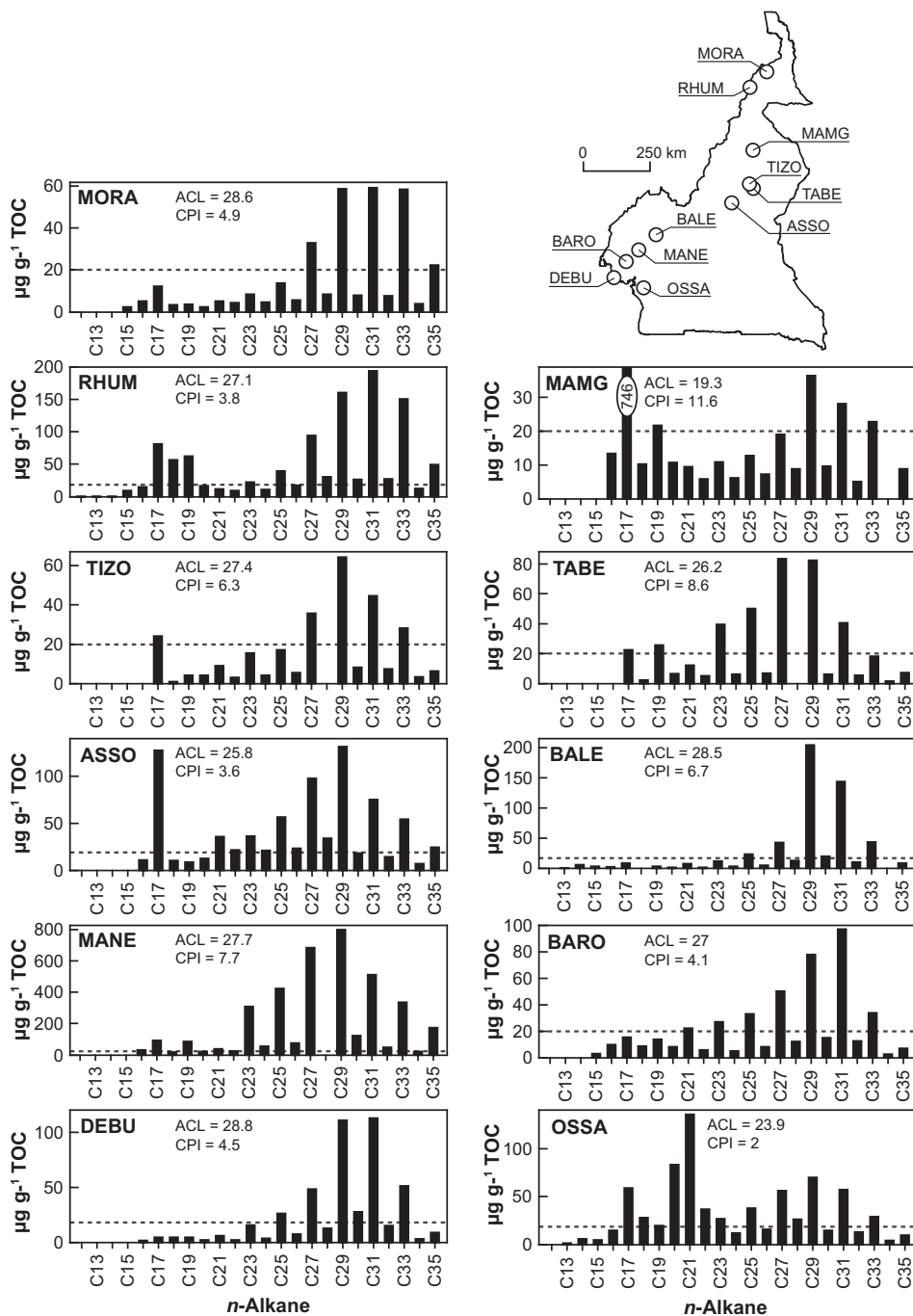


Fig. 4. Concentration, distribution, CPI (carbon predominance index = $\sum_{\text{odd}} C_n / \sum_{\text{even}} C_n$), and ACL (average chain length = $(\sum C_n \times n) / \sum C_n$) of *n*-alkanes in the lake surface sediments from Cameroon. The horizontal dashed line indicates a concentration of $20 \mu\text{g g}^{-1}$ TOC to compare the sites with each other. Inset map shows the location of the sampled lake basins.

terrestrial plants, with the predominance of long-chain odd numbered *n*-C₂₅ to *n*-C₃₃ alkanes (Fig. 5a). Similar distribution patterns of long-chain *n*-alkanes in topsoils and lake sediments (Fig. 5a and c) support an allochthonous source of these compounds as they originated from terrestrial plants (leaf waxes). The presence of short-chain *n*-C₁₆ to *n*-C₁₈ alkanes in topsoils, in low amounts relative to their long-chain homologues, suggests that sedimentary *n*-C₁₇ al-

kane may partly derive from terrestrial organisms. However, the relatively high abundance of *n*-C₁₇ alkane in the lake water POM (Fig. 5b) supports a major aquatic origin of this lipid biomarker in sediments (Han and Calvin, 1969; Gelpi et al., 1970; Cranwell et al., 1987; Meyers, 2003; Kristen et al., 2010). At virtually every site, the lake water POM was dominated by the *n*-C₂₃ alkane, which was likely produced by aquatic organisms, such as bryo-

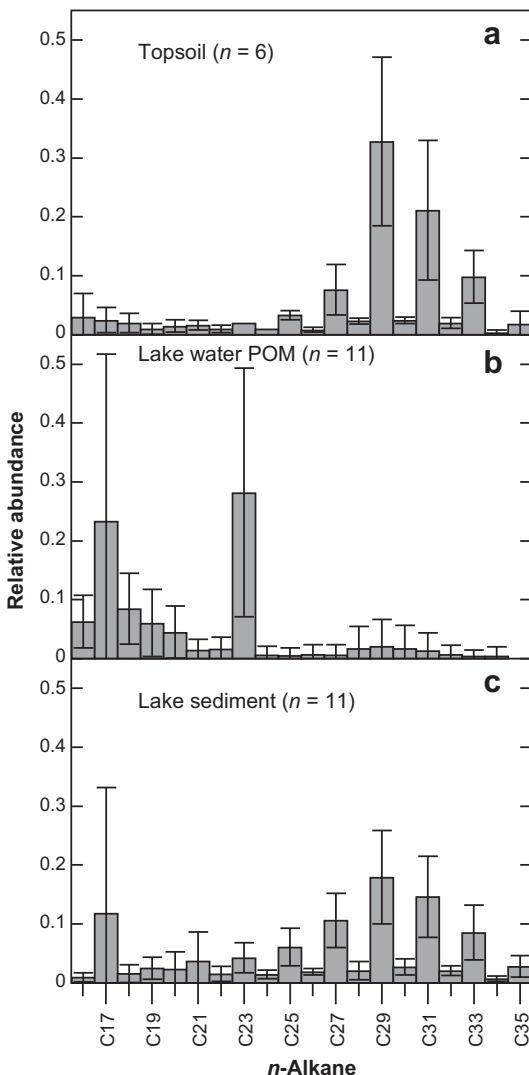


Fig. 5. Averaged histogram distribution (relative abundance normalised to sum of 1) of *n*-alkanes from (a) topsoil, (b) lake water particulate organic matter (POM), and (c) lake sediment. Number of sites sampled is given in parentheses. Error bars show the standard deviation.

phytes (*Sphagnum* sp.) and submerged macrophytes (Baas et al., 2000; Ficken et al., 2000; Mügler et al., 2008; Aichner et al., 2010a; Nichols et al., 2010; Sinnighe Damsté et al., 2011). The relatively low representation of *n*-C₂₃ alkane in lake sediments (Fig. 5c) suggests that either the production of this lipid biomarker is restricted in time and does not represent a significant contribution along the year or that its preservation in the sediment is poor.

The quasi-absence of long-chain *n*-alkanes in the lake water POM samples (significant amounts were only found for sites DEBU and MAMG) indicates that the transportation of leaf waxes from the catchments to the basin depocentres occurs during restricted soil erosion events induced by heavy rain; events that were not encountered during the fieldwork period (only possibly at site DEBU, which was sampled during a rainstorm). During such

events, the leaf waxes adsorbed onto the surfaces of relatively large soil/litter particles would sink rapidly to the lake bottoms, thus leaving the lake surface water depleted of long-chain *n*-alkanes. Moreover, the presence of numerous intact leaves floating at the surface of most of the sampled lakes suggests that a significant portion of the sedimentary leaf waxes originates from canopy leaves transported directly to the lakes by wind, followed by submergence and deposition at the lake bottoms. Such a transportation mechanism is relatively fast, resulting in insignificant time lags between leaf-wax synthesis on the catchments and deposition in lake sediments. Another mode of transport would be direct atmospheric deposition, which is potentially more important in the less vegetated sites in the north, but likely minor in the sites surrounded by dense rainforest in the south.

4.4. Sedimentary *n*-alkane δD values as proxies for source-water δD values in tropical Africa

To accurately reconstruct the δD values of past environmental waters, it is important to define the relationship between lipid biomarker δD values in modern sediments and the water δD values assimilated by the source organisms during lipid synthesis. Here, we focused on three lipid biomarkers: *n*-C₁₇, *n*-C₂₉, and *n*-C₃₁ alkanes, as they were the most common *n*-alkanes in the studied lake sediments. Moreover, these lipid biomarkers are of particular importance because they are extensively used as palaeohydrological and climate proxies. As shown in Fig. 3 and Table 4, the δD values of these three *n*-alkanes exhibited distinct patterns across the Cameroon transect, including differences in their absolute δD values along with divergences in the direction of changes with latitude.

We note that human activities (e.g., land clearance for agriculture) have altered the structure and composition of the local vegetation of some sampled sites. Although these alterations were limited for most of them, significant parts of the original forests at sites OSSA and BALE have been replaced by commercial tree plantations (i.e., oil palm and hevea at OSSA, and eucalyptus at BALE), which may complicate the comparison of these two sites with the others (see below).

4.4.1. *n*-C₁₇ alkane δD and $\delta^{13}C$ values

$\delta D_{n\text{-}C17}$ was not correlated with δD_{Sw} ($R^2 = 0.04$, $p < 0.5$) or with δD_{LK} ($R^2 = 0.01$, $p < 0.5$) in the sampled lakes in Cameroon (Table 5 and Fig. 6). These results are in contrast to observations from two transects in temperate regions of both Europe and North America, where sedimentary $\delta D_{n\text{-}C17}$ tracked changes in δD_{LK} with good accuracy (Huang et al., 2004; Sachse et al., 2004).

The lack of correlation between $\delta D_{n\text{-}C17}$ and δD_{LK} may be related to seasonal variations in δD_{LK} values, which have potentially affected the shallower lakes located to the drier north. Thus, if asynchronous and irregular phytoplankton blooms occurred at these lakes, algae and cyanobacteria would have sampled waters with different isotopic compositions, leading to a spurious relationship between

Table 4

δD values for the *n*-alkanes of interest together with calculated fractionations. Sites are presented from south to north reading from bottom to top, respectively.

Site code	<i>n</i> -Alkane δD values (‰)						Fractionation ε values (‰)					
	<i>n</i> -C ₁₇	SD	<i>n</i> -C ₂₉	SD	<i>n</i> -C ₃₁	SD	<i>n</i> -C ₁₇ /LK	<i>n</i> -C ₂₉ /SW	<i>n</i> -C ₂₉ /XW	<i>n</i> -C ₃₁ /LK	<i>n</i> -C ₃₁ / <i>n</i> -C ₂₉	LK/SW
MORA	-165	4	-170	3	-160	5	-175	-146	-147	-170	12	41
RHUM	-203	1	-167	3	-174	4	-203	-145	-138	-173	-8	26
MAMG	-115	8	-156	8	-160	5	-120	-141	-128	-165	-5	24
TIZO	-163	3	-155	1	-148	9	-182	-142	-138	-167	8	39
TABE	-156	1	-167	1	-158	5	-166	-154	-154	-167	11	27
ASSO	-120	1	-154	3	-174	3	-116	-141	-144	-170	-24	10
BALE	n.a.	n.a.	-150	1	-141	10	n.a.	-133	-133	-142	11	21
MANE	-160	3	-185	4	-178	8	-155	-152	-154	-173	9	34
BARO	n.a.	n.a.	-164	1	-166	4	n.a.	-151	-146	-168	-2	18
DEBU	-154	1	-153	5	-169	2	-147	-146	n.a.	-162	-19	0
OSSA	-191	3	-147	4	-150	7	-182	-136	n.a.	-140	-4	1
Mean	-159	—	-161	—	-162	—	-160	-144	-142	-168 ^a	-2 ^a	24 ^a
SD	29	—	11	—	12	—	29	7	9	4 ^a	13 ^a	13 ^a

n.a. = not available/not determined.

SD = standard deviation.

LK = lake water; SW = surface water; XW = xylem water.

^a Sites OSSA and BALE are excluded.

Table 5

Correlations (R^2 and *p*-values) and root-mean-square error of the residuals (RMSE) between *n*-alkane δD and source water δD , calculated via one-way analysis of variance (ANOVA).

	$\delta D_{n\text{-}C17}$				$\delta D_{n\text{-}C29}$				$\delta D_{n\text{-}C31}$			
	R^2	<i>p</i>	RMSE	<i>n</i>	R^2	<i>p</i>	RMSE	<i>n</i>	R^2	<i>p</i>	RMSE	<i>n</i>
δD_{SW}	0.04	<0.5	30.1	9	0.69	0.002	6.5	11	0.15	0.24	11.5	11
$\delta D_{\text{SW}}^{\text{a}}$	—	—	—	—	0.80	0.001	4.9	9	—	—	—	—
δD_{XW}	0.13	0.42	30.5	7	0.34	0.1	9.4	9	0.15	0.3	12.1	9
δD_{LK}	0.01	<0.5	30.4	9	0.013	<0.5	11.6	11	0.15	0.24	11.5	11
$\delta D_{\text{LK}}^{\text{a}}$	—	—	—	—	—	—	—	—	0.84	<0.001	4.1	9

LK = lake water; SW = surface water; XW = xylem water.

Bold values indicate a significant correlation within the 95% confidence interval ($p < 0.05$).

n = number of samples.

^a Sites OSSA and BALE are excluded.

$\delta D_{n\text{-}C17}$ (covering the last few years) and δD_{LK} (representing one single instant in time).

A second possible explanation may involve differences in the metabolic pathways of the organisms producing *n*-C₁₇ alkanes. Interestingly, the $\delta^{13}\text{C}_{n\text{-}C17}$ values from the Cameroon lake sediments showed large variations, ranging from -39 to -27‰ (Table 6 and Fig. 6). Sites MAMG, ASSO, and RHUM, which exhibited the most positive $\delta^{13}\text{C}_{n\text{-}C17}$ values (Fig. 6), also had the highest *n*-C₁₇ alkane concentrations (Fig. 4). Similar ranges in $\delta^{13}\text{C}_{n\text{-}C17}$ values (~10‰) have been observed in living cyanobacterial mats, aquatic plants, and surface sediments and have been related to different source organisms. Kristen et al. (2010) observed $\delta^{13}\text{C}_{n\text{-}C17}$ values of -35, -30, and -26‰ in floating cyanobacteria, lakeshore bacterial mats, and lake surface sediments, respectively, from a hypersaline lake in South Africa. van der Meer et al. (2000) reported $\delta^{13}\text{C}_{n\text{-}C17}$ values ranging from -36 to -34‰ for cyanobacteria living in a hot spring environment. Chikaraishi and Naraoka (2003)

noted heavier $\delta^{13}\text{C}_{n\text{-}C17}$ values, ranging from -24 to -23‰, for aquatic freshwater plants. Algae and photoautotrophic bacteria produce large amounts of *n*-C₁₇ alkane (Han and Calvin, 1969; Gelpi et al., 1970). However, heterotrophic bacteria and other heterotrophs, such as ciliated protozoa, may also produce significant amounts of this compound (Han and Calvin, 1969; Cranwell et al., 1987). Based on the large variability of $\delta^{13}\text{C}_{n\text{-}C17}$ values in the different source organisms, we conclude that the sedimentary $\delta^{13}\text{C}_{n\text{-}C17}$ values across Cameroon reflect diverse sources of the *n*-C₁₇ alkane, i.e., organisms with different metabolic pathways (e.g., photoautotrophs and heterotrophs). This conclusion is further supported by the lack of a significant relationship between $\delta D_{n\text{-}C17}$ and δD_{LK} as heterotrophs may use additional (organic) hydrogen sources. Moreover, recent work has shown that large variations in the δD values of lipids from heterotrophic organisms exist, probably due to differences in NADPH production pathways (Zhang et al., 2009).

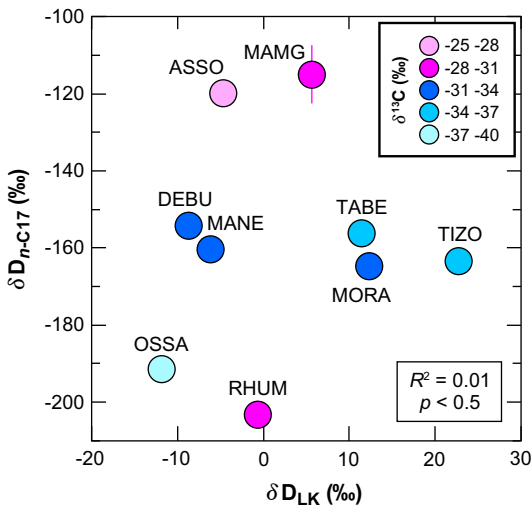


Fig. 6. Short-chain $n\text{-}C_{17}$ alkane δD vs. lake water δD (no significant correlation). The colour coding (upper-right box) corresponds to $\delta^{13}\text{C}$ values for $n\text{-}C_{17}$ alkane. (For interpretation of the references to colour in this figure legend, the reader is referred to the web version of this article.)

Table 6
 $\delta^{13}\text{C}$ values for the n -alkanes of interest. Sites are presented from south to north reading from bottom to top, respectively.

Site code	n -Alkane $\delta^{13}\text{C}$ values (‰)					
	$n\text{-}C_{17}$	SD	$n\text{-}C_{29}$	SD	$n\text{-}C_{31}$	SD
MORA	-33.1	0.7	-28.1	0.7	-30.1	0.1
RHUM	-30.7	0.4	-28.6	0.3	-29.7	0.3
MAMG	-30.7	2.2	-32.7	0.4	-32.1	0.3
TIZO	-35.9	0.3	-34.1	2.0	-33.2	0.7
TABE	-35.8	0.2	-32.1	0.2	-33.2	0.1
ASSO	-26.8	0.4	-32.9	0.2	-31.1	0.8
BALE	n.a.	n.a.	-37.5	0.4	-37.6	0.6
MANE	-33.7	0.8	-28.7	0.4	-28.1	0.3
BARO	n.a.	n.a.	-35.3	0.7	-36.2	0.4
DEBU	-33.0	0.7	-34.1	1.3	-36.8	0.4
OSSA	-39.1	1.1	-35.4	1.4	-39.0	1.8

n.a. = not available/not determined.

SD = standard deviation.

Our data emphasise that valuable information can be obtained from combined hydrogen and carbon isotope analysis. We suggest that such an approach may help identify different metabolic pathways and therefore ‘flag’ samples with substantial contributions by non-photoautotrophs. Notably, the δD and $\delta^{13}\text{C}$ values of the $n\text{-}C_{17}$ alkane from the MAMG and ASSO sites were the most positive and strongly divergent from other sites (Fig. 6), probably indicating substantial heterotrophic $n\text{-}C_{17}$ alkane sources at these sites.

As we found no significant correlation between $\delta D_{n\text{-}C17}$ and δD_{LK} in the Cameroon lake sediments, the analysis of more specific aquatic lipid biomarkers, such as dinosterol or botryococcene (cf. Gelpi et al., 1968; Volkman, 1986), may be more promising in palaeohydrological reconstructions for tropical systems.

4.4.2. $n\text{-}C_{29}$ alkane δD values as a proxy for surface water δD values

$\delta D_{n\text{-}C29}$ was significantly correlated with δD_{sw} ($R^2 = 0.69$, $p = 0.002$; Table 5 and Fig. 7a) across the Cameroon transect, illustrating that the isotopic composition of surface water exerted the primary control on the $n\text{-}C_{29}$ alkane δD values. The correlation between $\delta D_{n\text{-}C29}$ and δD_{sw} was not significant ($R^2 = 0.34$, $p = 0.1$; Table 5), which is a result that was probably related to the limited temporal integration of our xylem water δD values as these were sampled only at one point in time (Tables 3 and 5, and Fig. 3c). The $\delta D_{n\text{-}C29}$ values were not correlated with the δD_{LK} values ($R^2 = 0.013$, $p < 0.5$; Table 5).

The slope of the linear regression between $\delta D_{n\text{-}C29}$ and δD_{sw} (1.08) for the Cameroon lakes was slightly higher than a slope (0.86) obtained assuming a constant fractionation factor ($\alpha_{n\text{-}alkane/water}}$), but the intercept was comparable (-140 vs. -144‰; Fig. 7a). The small observed differences between the field-based and a one-component system (i.e., single hydrogen source) relationships could be related either to the limited number of data or to real differences between the sedimentary and surface water isotopic compositions, both of which integrated present-day environmental conditions over the past few years or less.

The apparent fractionation between $\delta D_{n\text{-}C29}$ and δD_{sw} ($\varepsilon_{n\text{-}C29/\text{sw}}$) ranged from -154 to -133‰ (Table 4). In theory, the apparent fractionation between the $\delta D_{n\text{-}C29}$ and δD of precipitation ($\varepsilon_{n\text{-}C29/\text{PW}}$) depends on several parameters, but mostly on soil-water (evaporation) and leaf-water (transpiration) D-enrichment as biosynthetic fractionation during lipid synthesis is thought to be constant (Sessions et al., 1999; Chikaraishi and Naraoka, 2003; Sachse et al., 2004, 2006; Smith and Freeman, 2006; Feakins and Sessions, 2010; McInerney et al., 2011). The observed $\varepsilon_{n\text{-}C29/\text{sw}}$ values from our sedimentary data fell within the range of the $\varepsilon_{n\text{-}C29/\text{PW}}$ values observed for C₃ and C₄ plants, although they were moderately larger (Chikaraishi and Naraoka, 2003; Sachse et al., 2006, 2010; Smith and Freeman, 2006; Hou et al., 2007; McInerney et al., 2011). It is possible that the larger $\varepsilon_{n\text{-}C29/\text{sw}}$ values suggest that the sampled surface waters along Cameroon were slightly evaporated and D-enriched relative to the original precipitation.

Due to lower mean annual relative humidity, leaf-water D-enrichment should be stronger in the drier north. However, the estimated $\varepsilon_{n\text{-}C29/\text{sw}}$ values across Cameroon remained relatively stable with changes in latitude (Table 4). In highly seasonal climate regimes as in the northern part of the Cameroon transect, it is expected that plants take advantage of the seasonal water availability during the rainy season and hence produce the majority of their leaf waxes during that season. Indeed, our data suggest that the $\delta D_{n\text{-}C29}$ values for the drier part of Cameroon were probably determined during the wet growing season, when small differences in relative humidity existed along the whole transect. Additionally, there is increasing evidence that leaf-wax n -alkanes in trees and grasses are mostly synthesised early in the ontogeny of a leaf (Sachse et al., 2010; Kahmen et al., 2011b), although seasonal variability of leaf-wax $\delta D_{n\text{-}alkane}$ values has been reported in temperate trees (Pedentchouk et al., 2008; Sachse et al.,

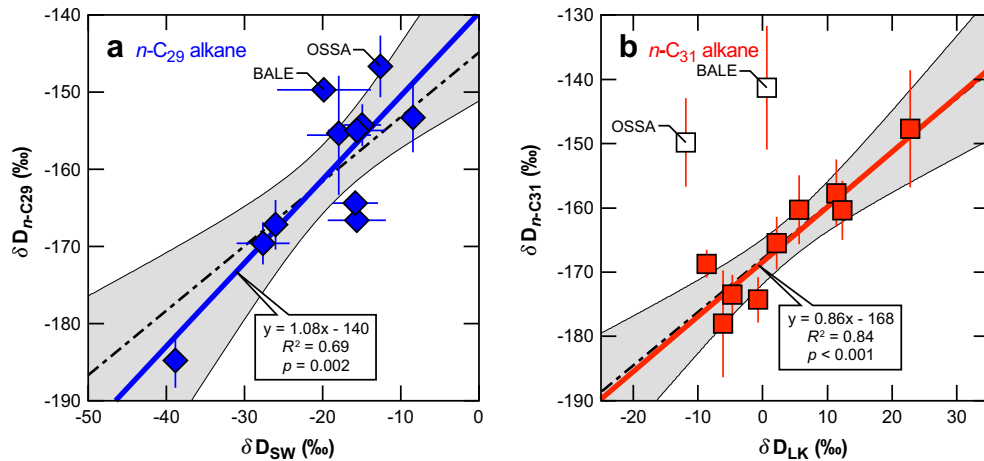


Fig. 7. Long-chain *n*-alkane δD vs. potential source-water δD . (a) $\delta D_{n\text{-}C29}$ vs. δD_{Sw} , blue line shows the linear regression (significant correlation). The correlation becomes more significant ($R^2 = 0.80, p = 0.001$) when sites OSSA and BALE are excluded; the natural vegetation at both sites has been strongly altered by human activities. (b) $\delta D_{n\text{-}C31}$ vs. δD_{LK} , red line shows the linear regression (significant correlation). Open symbols show sites OSSA and BALE not included in the evaluation (see main text). Thin black lines bounding grey areas represent the 95% confidence intervals of both regression lines. Black dashed lines show constant fractionation lines ($\delta D_{n\text{-}C29} = 0.86 \times \delta D_{\text{Sw}} - 144$, and $\delta D_{n\text{-}C31} = 0.83 \times \delta D_{\text{LK}} - 168$) calculated assuming a constant hydrogen isotope fractionation factor ($\alpha_{\text{n-alkane/water}}$) between $\delta D_{n\text{-}C29}$ and δD_{Sw} (average $\alpha = 0.86, n = 11$) and between $\delta D_{n\text{-}C31}$ and δD_{LK} (average $\alpha = 0.83, n = 9$). (For interpretation of the references to colour in this figure legend, the reader is referred to the web version of this article.)

2009). Consequently and due to the strong seasonality of climate in Cameroon, we interpret $\varepsilon_{n\text{-}C29/\text{SW}}$ being representative for growing season (wet season) climates rather than mean annual climate values.

In Cameroon, the composition of vegetation changes from dominantly C_3 trees and shrubs in the south to C_4 grasses in the north (Still and Powell, 2010). This vegetation gradient is reflected in the $\delta^{13}\text{C}$ values of long-chain *n*-alkanes. The $\delta^{13}\text{C}$ values of sedimentary long-chain *n*-alkanes ($n\text{-C}_{29}$ and $n\text{-C}_{31}$) ranged from -39 to $-28\text{\textperthousand}$ (Table 6). The lighter sedimentary $\delta^{13}\text{C}_{n\text{-alkane}}$ values were similar to the $\delta^{13}\text{C}_{n\text{-alkane}}$ values of C_3 rainforest plants (lianas, trees, and shrubs), while the heavier sedimentary $\delta^{13}\text{C}_{n\text{-alkane}}$ values corresponded to a mix between the $\delta^{13}\text{C}_{n\text{-alkane}}$ values of C_3 savanna plants (trees/shrubs) and C_4 savanna plants (grasses) (Rommerskirchen et al., 2006; Vogts et al., 2009). Hence, a change from C_3 -dominated to C_3/C_4 -mixed plants (from south to north) should also drive $\varepsilon_{n\text{-}C29/\text{SW}}$ to more negative values, with C_4 grasses having a $\sim 20\text{\textperthousand}$ larger apparent fractionation than C_3 trees/shrubs (Chikaraishi and Naraoka, 2003; Smith and Freeman, 2006; McInerney et al., 2011), thus counteracting any D-enrichment in the north.

Based on current estimates of biosynthetic fractionation, which range from -180 to $-150\text{\textperthousand}$ (i.e., Sessions et al., 1999; Sachse et al., 2004, 2010; Sessions, 2006; Feakins and Sessions, 2010; McInerney et al., 2011), we estimated a potential mean D-enrichment of soil/leaf water ranging from 0 to $+40\text{\textperthousand}$. The value of $\varepsilon_{n\text{-}C29/\text{SW}}$ ($-144 \pm 7\text{\textperthousand}$) was similar to the value of apparent fractionation between $n\text{-C}_{29}$ alkane and xylem water ($\varepsilon_{n\text{-}C29/\text{XW}} = -142 \pm 9\text{\textperthousand}$; Table 4). However, δD_{XW} was potentially affected by slight evaporative D-enrichment at some sites (see Section 4.1), suggesting that soil-water evaporation may have accounted for a part

of the estimated values of source-water D-enrichment (if significant) along the Cameroon transect. Conversely, the effect of leaf transpirational D-enrichment cannot be estimated with our data through the absence of growing season leaf water isotope measurements.

Importantly, the relative constancy of $\varepsilon_{n\text{-}C29/\text{SW}}$ values across the ecologically highly diverse Cameroon transect suggests that hydrogen isotopic compositions of sedimentary $n\text{-C}_{29}$ alkane may be used quantitatively to assess the hydrogen isotopic compositions of past surface waters in tropical Africa with an uncertainty of $\pm 10\text{\textperthousand}$ in both dry and wet regions.

4.4.3. $n\text{-C}_{31}$ alkane δD values as a proxy for lake water δD values

The $n\text{-C}_{31}$ alkane had a distinct hydrogen isotopic composition compared to the $n\text{-C}_{29}$ alkane for most sites, reflected by a poor correlation between $\delta D_{n\text{-}C29}$ and $\delta D_{n\text{-}C31}$ at the limit of statistical significance ($R^2 = 0.38, p = 0.044$; Fig. 8a). Although the $\delta D_{n\text{-}C29}$ and $\delta D_{n\text{-}C31}$ values revealed some variance with each other, they did not exhibit large offsets in mean absolute δD values ($-161 \pm 11\text{\textperthousand}$ and $-162 \pm 12\text{\textperthousand}$, respectively; Table 4). Surprisingly, $\delta D_{n\text{-}C31}$ showed a significant linear relationship with δD_{LK} ($R^2 = 0.84, p < 0.001$; Table 5), when excluding the two sites (OSSA and BALE) where pronounced human activities have altered the structure and composition of the local vegetation.

As shown in Fig. 7b, the slope of the linear regression between $\delta D_{n\text{-}C31}$ and δD_{LK} (0.86) was almost indistinguishable from the slope (0.83) when assuming a single hydrogen source system, and the intercept was identical ($-168\text{\textperthousand}$ for both). The observed significant correlation between $\delta D_{n\text{-}C31}$ and δD_{LK} is unexpected, and it implies that plants pro-

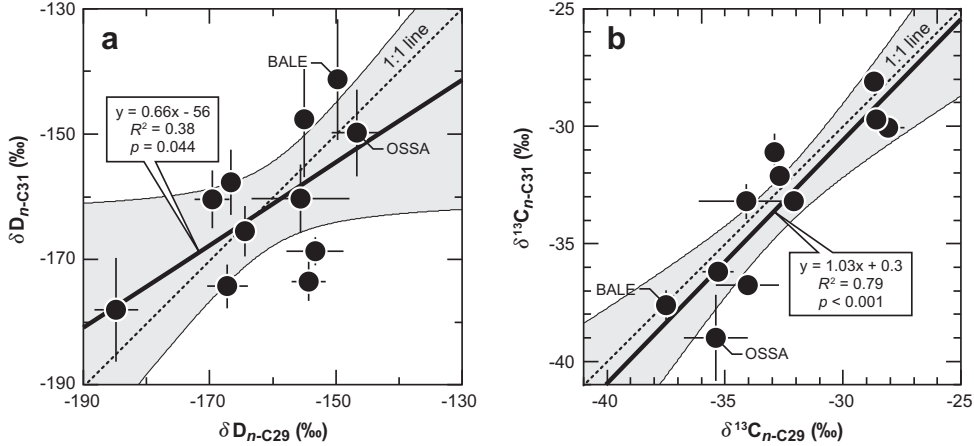


Fig. 8. δD and $\delta^{13}\text{C}$ values of $n\text{-C}_{29}$ and $n\text{-C}_{31}$ alkanes. (a) $\delta D_{n\text{-}C31}$ vs. $\delta D_{n\text{-}C29}$ (significant correlation). (b) $\delta^{13}\text{C}_{n\text{-}C31}$ vs. $\delta^{13}\text{C}_{n\text{-}C29}$ (significant correlation). Thin black lines bounding grey areas represent the 95% confidence intervals of the regression lines (thick black lines). Diagonal dotted lines represent the one-to-one relationship.

ducing $n\text{-C}_{31}$ alkanes along the Cameroon transect derived their source water either from lakes or similarly evaporated water pools, i.e., waters that clearly diverged from surface waters. As such, our data suggest that different plants, which were taking up water of different isotopic compositions, produced different long-chain n -alkane homologues. These distinct water pools were either non-evaporated or evaporated.

The differences between the $\delta D_{n\text{-}C29}$ and $\delta D_{n\text{-}C31}$ values are in contrast with observations from mid- and high-latitude sites and from high-elevation sites, where the hydrogen isotopic composition of long-chain n -alkane homologues from sediment, soil, and plant samples were generally well correlated with each other (e.g., Sachse et al., 2004; Bi et al., 2005; Smith and Freeman, 2006; Hou et al., 2007; Rao et al., 2009; Polissar and Freeman, 2010). However, significant variability in the δD values between long-chain n -alkanes has been previously described within single plant species and in different seasons and was explained by differences in the timing of production of the different carbon-numbered homologues in combination with a fast turnover rate of n -alkyl compounds on time scales of less than a month (Sessions, 2006; Pedentchouk et al., 2008; Sachse et al., 2009).

The significant correlation between $\delta^{13}\text{C}_{n\text{-}C29}$ and $\delta^{13}\text{C}_{n\text{-}C31}$ ($R^2 = 0.79$, $p < 0.001$) and the slope of the linear relation (1.03) identical to the 1:1 line (Fig. 8b) suggests that for each studied site across Cameroon, the plants that either produced the $n\text{-C}_{29}$ or the $n\text{-C}_{31}$ alkanes used the same photosynthetic pathways. Thus, variations in plant photosynthetic pathways (i.e., C₃ vs. C₄) cannot account for the observed variations in δD values between the two sedimentary n -alkane homologues.

The premise that distinct water isotopic compositions were recorded by both $n\text{-C}_{29}$ and $n\text{-C}_{31}$ alkanes remains highly ambiguous, and we currently do not have sufficient data to resolve the specific factors responsible for the observed isotopic differences. However, below, we explore hypotheses that may help explain our observations.

Although δD values from plant-derived n -alkanes from tropical Africa are not available, several studies investigating n -alkane distribution patterns and stable carbon isotopic compositions exist. Rommerskirchen et al. (2006) and Vogts et al. (2009) showed that $n\text{-C}_{29}$ and $n\text{-C}_{31}$ alkanes are present in almost all the African plants analysed and that they are generally the most abundant n -alkanes. How-

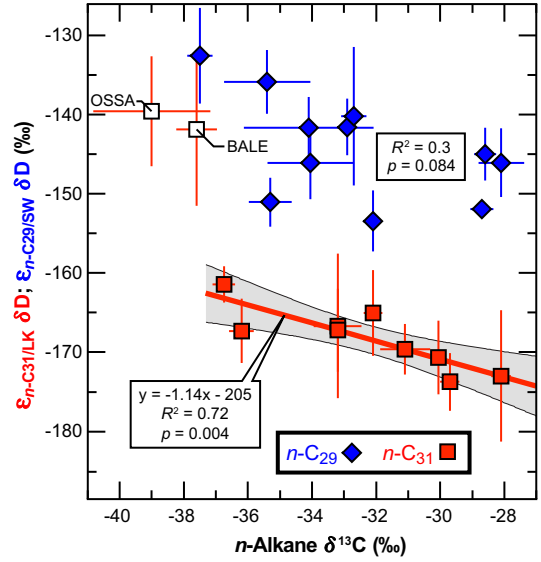


Fig. 9. Influence of photosynthetic pathways on apparent fractionation between n -alkane δD and source-water δD . Blue diamonds: apparent fractionation between $\delta D_{n\text{-}C29}$ and δD_{SW} ($\varepsilon_{n\text{-}C29/\text{SW}}$) vs. $\delta^{13}\text{C}_{n\text{-}C29}$ (no significant correlation). Red squares: apparent fractionation between $\delta D_{n\text{-}C31}$ and δD_{LK} ($\varepsilon_{n\text{-}C31/\text{LK}}$) vs. $\delta^{13}\text{C}_{n\text{-}C31}$ (significant correlation). Open symbols show sites OSSA and BALE not included in the evaluation (see main text). Thin black lines bounding the grey area represent the 95% confidence intervals of the regression line (in red). (For interpretation of the references to colour in this figure legend, the reader is referred to the web version of this article.)

ever, a large variability of *n*-C₂₉ vs. *n*-C₃₁ alkane distribution was found among different plant subspecies, with *n*-C₂₉ dominating in certain plants, while *n*-C₃₁ accounted for only minor contributions and vice versa (Rommerskirchen et al., 2006; Vogts et al., 2009; Kristen et al., 2010). Although we have no data on *n*-alkane distributions of the lake catchment vegetation, it is theoretically possible that plants producing predominantly the *n*-C₂₉ alkane may inhabit areas away from the lake's influence and that plants producing predominantly the *n*-C₃₁ alkane may inhabit lakeshore environments (e.g., riparian and/or aquatic plants) and derive their water directly from the evaporated lake.

A comparison of the apparent fractionation between *n*-alkane δD and source water δD with *n*-alkane $\delta^{13}\text{C}$ further demonstrates the potential links between the photosynthetic pathway (and associated plant growth form) and the differential D-enrichment (Fig. 9). The $\varepsilon_{n\text{-C}31}/\text{LK}$ and $\delta^{13}\text{C}_{n\text{-C}31}$ values exhibited a significant negative linear correlation ($R^2 = 0.712$, $p = 0.004$). This relationship accounted for a difference of $\sim 10\text{\textperthousand}$ in $\varepsilon_{n\text{-C}31}/\text{LK}$ values for

$\delta^{13}\text{C}_{n\text{-C}31}$ values ranging from -37 to $-28\text{\textperthousand}$. This result may be related to the observed difference in apparent fractionation between C₃ plants (mostly dicots) vs. C₄ plants (mostly monocots) (Chikaraishi and Naraoka, 2003; Smith and Freeman, 2006; McInerney et al., 2011).

Currently, more data on the nature, production, age, and dispersion of leaf-wax *n*-alkanes from the dominant plant species occupying each of the investigated tropical ecosystems are needed for an unambiguous evaluation of the causal relationship between $\delta D_{n\text{-C}31}$ and δD_{LK} . Although the mechanism behind this relationship is not understood, the significant correlation between $\delta D_{n\text{-C}31}$ and δD_{LK} as well as the stable $\varepsilon_{n\text{-C}31}/\text{LK}$ values with changes in latitude (Table 4) suggest that $\delta D_{n\text{-C}31}$ could be a reliable proxy of δD_{LK} for strongly contrasting ecosystems in tropical Africa.

4.4.4. A possible higher plant-based evaporation proxy

As discussed above, $\delta D_{n\text{-C}29}$ was significantly correlated with δD_{SW} , while $\delta D_{n\text{-C}31}$ was significantly correlated with δD_{LK} . Consequently, the offset between $\delta D_{n\text{-C}31}$ and

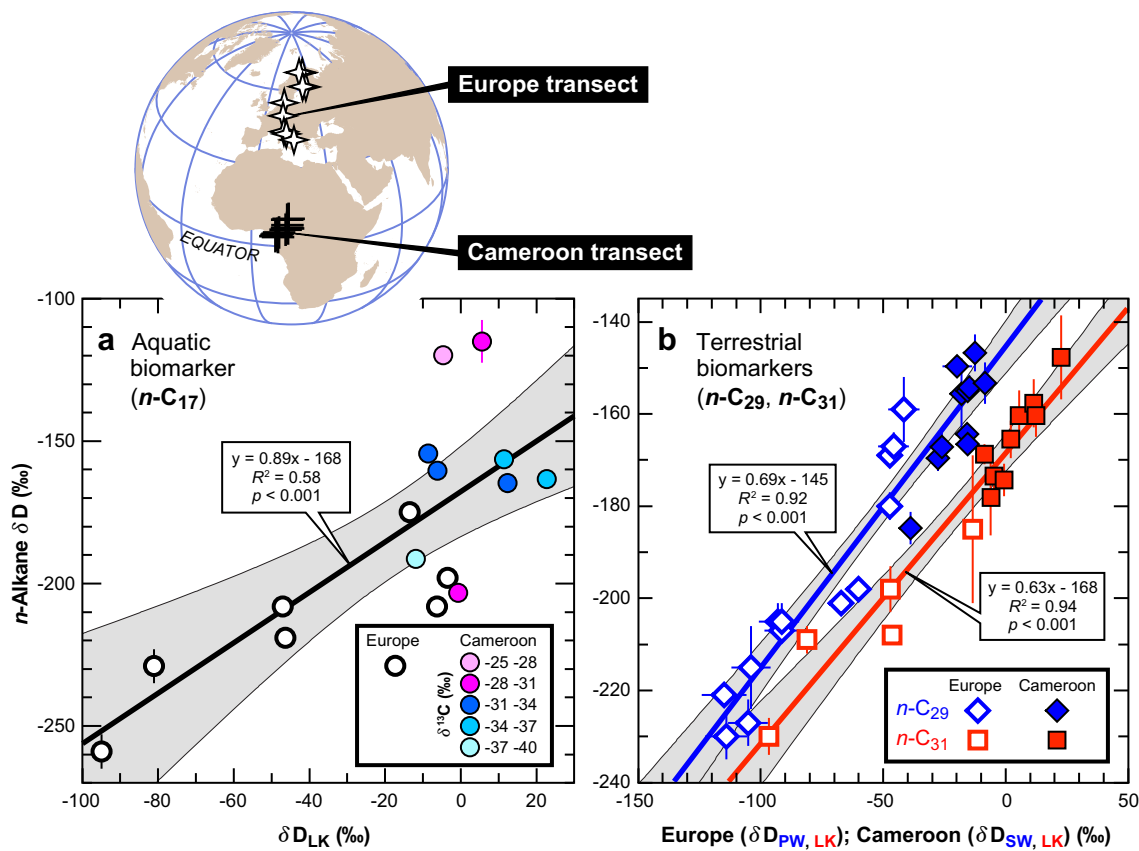


Fig. 10. *n*-Alkane δD hemispheric calibrations: comparison of lake surface sediment data from Cameroon (this study) and Europe (Sachse et al., 2004). (a) 'Aquatic biomarker' $\delta D_{n\text{-C}17}$ vs. δD_{LK} . White circles show data from Europe. Coloured circles show data from Cameroon. Colour coding (lower-right box) corresponds to the $\delta^{13}\text{C}_{n\text{-C}17}$ values. The thick black line is the resulting hemispheric regression line (significant correlation). (b) 'Terrestrial biomarkers' *n*-C₂₉ and *n*-C₃₁ alkane δD vs. source-water δD . The blue line passing through the blue diamonds is the hemispheric regression line resulting from the combination of $\delta D_{n\text{-C}29}$ vs. δD_{SW} for Cameroon and of $\delta D_{n\text{-C}29}$ vs. δD_{PW} for Europe (significant correlation). The red line passing through the red squares is the hemispheric regression line of $\delta D_{n\text{-C}31}$ vs. δD_{LK} (significant correlation). Open symbols: Europe data, filled symbols: Cameroon data. Thin black lines bounding grey areas represent the 95% confidence intervals of the regression lines. Inset map shows sites from the Cameroon and Europe transects (black crosses and white stars, respectively).

$\delta D_{n\text{-}C29}$ ($\varepsilon_{n\text{-}C31/n\text{-}C29}$) should represent the local lake water balance (evaporation/precipitation) expressed as the offset between δD_{LK} and δD_{SW} ($\varepsilon_{LK/SW}$). Indeed, we found that $\varepsilon_{n\text{-}C31/n\text{-}C29}$ was significantly correlated with $\varepsilon_{LK/SW}$ ($R^2 = 0.76$, $p = 0.002$). The $\varepsilon_{n\text{-}C31/n\text{-}C29}$ values ranged from -24 to $+12\text{‰}$, while the $\varepsilon_{LK/SW}$ values ranged from 0 to $+41\text{‰}$ (Table 4).

Similar approaches relying on ‘offsets’ in the δD values of *n*-alkane homologues have been described for both lake and bog sediments in Europe, North America, and the Tibetan Plateau (Sachse et al., 2004; Mügler et al., 2008; Aichner et al., 2010b; Nichols et al., 2010). The results from the Cameroon transect demonstrate the possible applicability of $\varepsilon_{n\text{-}C31/n\text{-}C29}$ as a proxy for an evaporation/precipitation balance in tropical Africa. This approach has the advantage that potential changes in the moisture source can be separated from changes in evaporation, and therefore, it holds great potential for palaeohydrological reconstructions. However, due to the lack of a mechanistic understanding of the cause for the observed offset, this new higher plant-based proxy should be used with care, and additional detailed ecosystem-level studies are needed to support its application in the lacustrine environments throughout tropical Africa.

4.5. *n*-Alkane δD calibrations: a hemispheric perspective

By combining our new data from Cameroon with previously published data from a surface sediment transect across Europe (Sachse et al., 2004), we are able to evaluate the robustness of *n*-alkane δD as a proxy of source water δD at hemispheric scale (Fig. 10).

Although the $\delta D_{n\text{-}C17}$ values from the Cameroon lakes did not correlate with δD_{LK} , combining the $\delta D_{n\text{-}C17}$ values for both transects resulted in a significant correlation between $\delta D_{n\text{-}C17}$ and δD_{LK} ($R^2 = 0.58$, $p < 0.001$, $n = 16$; Fig. 10a). The equation of the linear regression ($\delta D_{n\text{-}C17} = 0.89 \times \delta D_{LK} - 168$) was nearly identical to the linear regression obtained on the same lipid biomarker from a lake transect across North America ($\delta D_{n\text{-}C17} = 0.87 \times \delta D_{LK} - 155$) (Huang et al., 2004). Taken together, these data suggest that $\delta D_{n\text{-}C17}$ is a potential proxy for δD_{LK} for the highly contrasted ecosystems of the northern hemisphere. However, the apparent scatter of the data along the composite linear regression emphasises possible limitations for a universal application of this δD_{LK} proxy. Strikingly, the Cameroon data, which diverged the most from the composite linear regression, had the most positive $\delta^{13}\text{C}_{n\text{-}C17}$ values. This result indicates that heterotrophic organisms may have contributed to sedimentary *n*- C_{17} alkane accumulations and therefore, derived their hydrogen from different sources, especially in tropical ecosystems (see Section 4.4.1).

Concerning the *n*- C_{29} alkane, an evaluation of the isotopic relationships between $\delta D_{n\text{-}C29}$ and δD_{SW} (surface water, Cameroon transect) and δD_{PW} (precipitation, Europe transect) over hemispheric scale resulted in a significant correlation ($R^2 = 0.92$, $p < 0.001$, $n = 24$; Fig. 10b), again highlighting the robustness of this proxy in ecosystems spanning tropical rainforests, savannas, and temperate to boreal forests. Concerning the *n*- C_{31} alkane, the correlation

between $\delta D_{n\text{-}C31}$ and δD_{LK} also remained significant when combining the data of Cameroon and Europe ($R^2 = 0.94$, $p < 0.001$; $n = 14$; Fig. 10b).

5. CONCLUSIONS

Our survey of *n*-alkane δD values from the surface sediments of 11 lakes across Cameroon reveals new insights into the relationships between the hydrogen isotope ratios of *n*-alkanes and the hydrogen isotope ratios of source waters in tropical regions. Our study also highlights that a robust database of source water δD values (lake water, river water, groundwater, precipitation, and plant water) is essential to understand the links between the δD values of sedimentary lipid biomarkers and their respective hydrogen sources.

We find no significant correlation between the $\delta D_{n\text{-}C17}$ and lake water δD (δD_{LK}) in the Cameroon lakes. Large variations in $\delta^{13}\text{C}_{n\text{-}C17}$ values point to various source organisms with diverse metabolic pathways (e.g., photo-autotrophs vs. heterotrophs) for the *n*- C_{17} alkane.

We demonstrate that $\delta D_{n\text{-}C29}$ was significantly correlated with surface water δD (δD_{SW}). Surface waters are likely similar to precipitation in most cases, but they can be locally altered by moderate evaporation processes. Our results validate the use of $\delta D_{n\text{-}C29}$ as a robust proxy for the isotopic composition of surface water in tropical Africa.

Conversely, $\delta D_{n\text{-}C31}$ was distinct from $\delta D_{n\text{-}C29}$ and was not correlated with δD_{SW} but instead was correlated with δD_{LK} . This result suggests that the plants producing the *n*- C_{31} alkane derived their water from a different source than the *n*- C_{29} alkane-producing plants. We hypothesise that while the *n*- C_{29} alkane originated from terrestrial plants occupying catchment areas, the *n*- C_{31} alkane originated from plants inhabiting the lakeshore environments.

We also find evidence for plant physiological processes affecting leaf-wax δD values along the investigated large environmental gradient. The significant correlation between $\varepsilon_{n\text{-}C31/LK}$ and $\delta^{13}\text{C}_{n\text{-}C31}$ suggests that a change from a C_3 -dominated tree/shrub vegetation to a C_3/C_4 -mixed shrub/grass vegetation accounted for a $\sim 10\text{‰}$ D-depletion in $\delta D_{n\text{-}C31}$ values.

Furthermore, because $\delta D_{n\text{-}C29}$ was significantly correlated with δD_{SW} and $\delta D_{n\text{-}C31}$ with δD_{LK} , we propose that the offset between $\delta D_{n\text{-}C31}$ and $\delta D_{n\text{-}C29}$ ($\varepsilon_{n\text{-}C31/n\text{-}C29}$) could be a valuable indicator to estimate the local evaporation/precipitation balance if the mechanistic basis for these observations can eventually be elucidated.

Our data suggest that differences in metabolic pathways (e.g., for bacteria/algae) and in photosynthetic pathways and associated growth forms (e.g., for plants) may result in the assimilation of different hydrogen pools by the source organisms. We therefore recommend the use of unambiguous lipid biomarkers and/or a dual isotopic approach (hydrogen and carbon) to identify these mechanisms.

Importantly, the integration of our new data from Cameroon with previously published data from Europe clearly shows that the δD values of long-chain *n*-alkanes (C_{29} and C_{31}) are excellent proxies for the δD values of source waters (i.e., surface water and precipitation as well as lake

water) across large environmental gradients representative of the entire northern hemisphere.

ACKNOWLEDGMENTS

This research was supported by the German Science Foundation (DFG) to Y.G. (GA-1629/1-1) and through the DFG Emmy-Noether Programme to D.S. (SA-1889/1-1), the DFG Leibniz Center for Surface Process and Climate Studies at Potsdam University (to Y.G. and D.S.), and the MPI-BGC Jena for additional funding (to V.F.S. and G.G.). We thank S. Rühlow for the IRMS analytical assistance, H. Geilmann for measurements of the δD and $\delta^{18}\text{O}$ values of the water samples, and A. Musiol for measurements of the TOC of the sediment samples. We would also like to thank M.R. Strecker for his continuous support throughout this study and E. Schefuß for discussions. We thank A.L. Sessions, two anonymous reviewers, and J.S. Sinnenhe Damsté for helpful suggestions that greatly improved this manuscript. We are particularly indebted to the Ministry of Scientific Research and Innovation of Cameroon for providing research permits (54/MINRESI/B00/C00/C10/C13). We are grateful to the Institut de Recherche pour le Développement (IRD) for logistical support. Finally, the population, administrative authorities, and traditional chiefs of Cameroon are warmly acknowledged for their support and collaboration during the fieldwork.

APPENDIX A. SUPPLEMENTARY DATA

Supplementary data associated with this article can be found, in the online version, at doi:10.1016/j.gca.2011.11.039.

REFERENCES

- Aichner B., Herzsuh U. and Wilkes H. (2010a) Influence of aquatic macrophytes on the stable carbon isotopic signatures of sedimentary organic matter in lakes on the Tibetan Plateau. *Org. Geochem.* **41**, 706–718.
- Aichner B., Herzsuh U., Wilkes H., Vieth A. and Bohner J. (2010b) δD values of *n*-alkanes in Tibetan lake sediments and aquatic macrophytes – A surface sediment study and application to a 16 ka record from Lake Koucha. *Org. Geochem.* **41**, 779–790.
- Ako A. A., Shimada J., Ichianagi K., Koike K., Hosono T., Eyoung G. E. T. and Iskandar I. (2009) Isotope Hydrology and Hydrochemistry of Water Resources in the Banana Plain (Mungo-Division) of the Cameroon Volcanic Line. *J. Environ. Hydrol.* **17**, 1–20.
- Andersen N., Paul H. A., Bernasconi S. M., McKenzie J. A., Behrens A., Schaeffer P. and Albrecht P. (2001) Large and rapid climate variability during the Messinian salinity crisis: evidence from deuterium concentrations of individual biomarkers. *Geology* **29**, 799–802.
- Baas M., Pancost R., van Geel B. and Sinnenhe Damsté J. S. (2000) A comparative study of lipids in *Sphagnum* species. *Org. Geochem.* **31**, 535–541.
- Barker P. A., Leng M. J., Gasse F. and Huang Y. S. (2007) Century-to-millennial scale climatic variability in Lake Malawi revealed by isotope records. *Earth Planet. Sci. Lett.* **261**, 93–103.
- Barnes C. J. and Allison G. B. (1988) Tracing of water movement in the unsaturated zone using stable isotopes of hydrogen and oxygen. *J. Hydrol.* **100**, 143–176.
- Bi X., Sheng G., Liu X., Li C. and Fu J. (2005) Molecular and carbon and hydrogen isotopic composition of *n*-alkanes in plant leaf waxes. *Org. Geochem.* **36**, 1405–1417.
- Birkett C., Murtugudde R. and Allan T. (1999) Indian Ocean climate event brings floods to East Africa's lakes and the Sudd marsh. *Geophys. Res. Lett.* **26**, 1031–1034.
- Bowen G. J. and Revenaugh J. (2003) Interpolating the isotopic composition of modern meteoric precipitation. *Water Resour. Res.* **39**, 1299. doi:10.1029/2003WR002086.
- Brand W. A., Geilmann H., Crosson E. R. and Rella C. W. (2009) Cavity ring-down spectroscopy versus high-temperature conversion isotope ratio mass spectrometry; a case study on $\delta^2\text{H}$ and $\delta^{18}\text{O}$ of pure water samples and alcohol/water mixtures. *Rapid Commun. Mass Spectrom.* **23**, 1879–1884.
- Burgoyne T. W. and Hayes J. M. (1998) Quantitative production of H_2 by pyrolysis of gas chromatographic effluents. *Anal. Chem.* **70**, 5136–5141.
- Cane M. A. (2005) The evolution of El Niño, past and future. *Earth Planet. Sci. Lett.* **230**, 227–240.
- Chikaraishi Y. and Naraoka H. (2003) Compound-specific δD – $\delta^{13}\text{C}$ analyses of *n*-alkanes extracted from terrestrial and aquatic plants. *Phytochemistry* **63**, 361–371.
- CIEH (1990) Annales des Précipitations Journalières de 1966 à 1980. CIEH–ASECNA–ORSTOM, Paris, France.
- Craig H. (1961) Isotopic variations in meteoric waters. *Science* **133**, 1702–1703.
- Craig H. and Gordon L. I. (1965) Deuterium and oxygen 18 variations in the ocean and marine atmosphere. In *Stable Isotopes in Oceanographic Studies and Paleotemperatures* (ed. E. Tongiorgi). Lab. di Geologia Nucleare, Pisa, Italia, pp. 9–130.
- Cranwell P. A., Eglington G. and Robinson N. (1987) Lipids of aquatic organisms as potential contributors to lacustrine sediments–II. *Org. Geochem.* **11**, 513–527.
- Dansgaard W. (1964) Stable isotopes in precipitation. *Tellus* **16**, 436–468.
- Dawson T. E. and Ehleringer J. R. (1991) Streamside trees that do not use stream water. *Nature* **350**, 335–337.
- de Wit M. and Stankiewicz J. (2006) Changes in surface water supply across Africa with predicted climate change. *Science* **311**, 1917–1921.
- Delalande M. (2008) Hydrologie et géochimie isotopique du lac Masoko et des lacs volcaniques de la province active du Rungwe (Sud-Ouest Tanzanie). Ph. D. thesis, Univ. Paris Sud, Orsay, France.
- Eglington G. and Hamilton R. J. (1967) Leaf Epicuticular Waxes. *Science* **156**, 1322–1334.
- Fantong W. Y., Satake H., Ako F. T., Ayonghe S. N., Asai K., Mandal A. K. and Ako A. A. (2010) Hydrochemical and isotopic evidence of recharge, apparent age, and flow direction of groundwater in Mayo Tsanaga River Basin, Cameroon: bearings on contamination. *Environ. Earth Sci.* **60**, 107–120.
- Feehins S. J. and Sessions A. L. (2010) Controls on the D/H ratios of plant leaf waxes in an arid ecosystem. *Geochim. Cosmochim. Acta* **74**, 2128–2141.
- Ficken K. J., Li B., Swain D. L. and Eglington G. (2000) An *n*-alkane proxy for the sedimentary input of submerged/floating freshwater aquatic macrophytes. *Org. Geochem.* **31**, 745–749.
- Fontes J. C. and Olivry J. C. (1976) Premiers résultats sur la composition isotopique des précipitations de la région du Mont Cameroun. *Cah. ORSTOM, sér. Hydrol.* **13**, 179–194.
- Gat J. R. and Gonfiantini R. (1981) Stable Isotope Hydrology: deuterium and Oxygen-18 in the Water Cycle. IAEA, Technical Reports Series No. 210, Vienna.
- Gehre M., Geilmann H., Richter J., Werner R. A. and Brand W. A. (2004) Continuous flow $^2\text{H}/^1\text{H}$ and $^{18}\text{O}/^{16}\text{O}$ analysis of water

- samples with dual inlet precision. *Rapid Commun. Mass Spectrom.* **18**, 2650–2660.
- Gelpi E., Oró J., Schneider H. J. and Bennett E. O. (1968) Olefins of high molecular weight in two microscopic algae. *Science* **161**, 700–701.
- Gelpi E., Schneider H., Mann J. and Oró J. (1970) Lipids of Geochemical Significance in Microscopic Algae, Part I: Hydrocarbons of Geochemical Significance in Microscopic Algae. *Phytochemistry* **9**, 603–612.
- Giger W., Schaffner C. and Wakeham S. G. (1980) Aliphatic and olefinic hydrocarbons in recent sediments of Greifensee, Switzerland. *Geochim. Cosmochim. Acta* **44**, 119–129.
- Grice K., de Mesmay R., Glucina A. and Wang S. (2008) An improved and rapid 5A molecular sieve method for gas chromatography isotope ratio mass spectrometry of *n*-alkanes (C_8 – C_{30+}). *Org. Geochem.* **39**, 284–288.
- Han J. and Calvin M. (1969) Hydrocarbon distribution of algae and bacteria, and microbiological activity in sediments. *Proc. Natl. Acad. Sci. U. S. A.* **64**, 436–443.
- Hijmans R. J., Cameron S. E., Parra J. L., Jones P. G. and Jarvis A. (2005) Very high resolution interpolated climate surfaces for global land areas. *Int. J. Climatol.* **25**, 1965–1978.
- Hilkert A. W., Douthitt C. B., Schluter H. J. and Brand W. A. (1999) Isotope ratio monitoring gas chromatography mass spectrometry of D/H by high temperature conversion isotope ratio mass spectrometry. *Rapid Commun. Mass Spectrom.* **13**, 1226–1230.
- Hoke G. D., Garzione C. N., Araneo D. C., Latorre C., Strecker M. R. and Williams K. J. (2009) The stable isotope altimeter: Do Quaternary pedogenic carbonates predict modern elevations? *Geology* **37**, 1015–1018.
- Hou J., D'Andrea W. J., MacDonald D. and Huang Y. (2007) Hydrogen isotopic variability in leaf waxes among terrestrial and aquatic plants around Blood Pond, Massachusetts (USA). *Org. Geochem.* **38**, 977–984.
- Hou J., D'Andrea W. J. and Huang Y. (2008) Can sedimentary leaf waxes record D/H ratios of continental precipitation? Field, model, and experimental assessments. *Geochim. Cosmochim. Acta* **72**, 3503–3517.
- Huang Y., Shuman B., Wang Y. and Webb T. (2002) Hydrogen isotope ratios of palmitic acid in lacustrine sediments record late Quaternary climate variations. *Geology* **30**, 1103–1106.
- Huang Y., Shuman B., Wang Y. and Webb T. (2004) Hydrogen isotope ratios of individual lipids in lake sediments as novel tracers of climatic and environmental change: a surface sediment test. *J. Paleolimnol.* **31**, 363–375.
- IAEA/WMO (2006) Global network of isotopes in precipitation: the GNIP database. International Atomic Energy Agency–World Meteorological Organization, <http://nds121.iaea.org/wiser/>.
- Jouzel J., Hoffmann G., Koster R. D. and Masson V. (2000) Water isotopes in precipitation: data/model comparison for present-day and past climates. *Quat. Sci. Rev.* **19**, 363–379.
- Kahmen A., Sachse D., Arndt S. K., Tu K. P., Farrington H., Vitousek P. M. and Dawson T. E. (2011a) Cellulose $\delta^{18}\text{O}$ is an index of leaf-to-air vapor pressure difference (VPD) in tropical plants. *Proc. Natl. Acad. Sci. U. S. A.* **108**, 1981–1986.
- Kahmen A., Dawson T. E., Vieth A. and Sachse D. (2011b) Leaf wax n-alkane δD values are determined early in the ontogeny of *Populus trichocarpa* leaves when grown under controlled environmental conditions. *Plant Cell Environ.* **34**, 1639–1651.
- Kebede S., Lamb H., Telford R., Leng M. and Umer M. (2004) Lake - groundwater relationships, oxygen isotope balance and climate sensitivity of the Bishoftu Crater Lakes, Ethiopia. In *The East African Great Lakes: Limnology, Palaeolimnology and Biodiversity* (eds. E. Odada and D. Olago). Springer, Dordrecht, The Netherlands, pp. 261–275.
- Kendall C. and Coplen T. B. (2001) Distribution of oxygen-18 and deuterium in river waters across the United States. *Hydrolog. Process.* **15**, 1363–1393.
- Ketchemen B., Naah E., Faye A. and Aranyossy J. F. (1993) Application des Isotopes de l'Environnement à l'Etude des Aquifères du Grand Yaéré (Extrême Nord du Cameroun). In *Les Ressources en Eau du Sahel: Etudes Hydrogéologiques et Hydrologiques en Afrique de l'Ouest par les Techniques Isotopiques*. AIEA, TECDOC-721, Vienna, Austria, pp. 107–122.
- Kling G. W. (1988) Comparative transparency, depth of mixing, and stability of stratification in lakes of Cameroon, West Africa. *Limnol. Oceanogr.* **33**, 27–40.
- Kohn M. J., Schoeninger M. J. and Valley J. W. (1996) Herbivore tooth oxygen isotope compositions: effects of diet and physiology. *Geochim. Cosmochim. Acta* **60**, 3889–3896.
- Kristen I., Wilkes H., Vieth A., Zink K. G., Plessen B., Thorpe J., Partridge T. C. and Oberhansli H. (2010) Biomarker and stable carbon isotope analyses of sedimentary organic matter from Lake Tswaing: evidence for deglacial wetness and early Holocene drought from South Africa. *J. Paleolimnol.* **44**, 143–160.
- Lachnit M. S. and Patterson W. P. (2002) Stable isotope values of Costa Rican surface waters. *J. Hydrol.* **260**, 135–150.
- Lamb H., Kebede S., Leng M., Ricketts D., Telford R. and Umer M. (2004) Origin and isotopic composition of Aragonite Laminae in an Ethiopian Crater Lake. In *The East African Great Lakes: Limnology, Palaeolimnology and Biodiversity* (eds. E. Odada and D. Olago). Springer, Dordrecht, The Netherlands, pp. 487–508.
- Lefèvre R. (1967) Aspect de la pluviométrie dans la région du mont Cameroun. *Cah. ORSTOM, sér. Hydrol.* **4**, 15–43.
- Leng M. J. (ed.) (2006) *Isotopes in Palaeoenvironmental Research*. Springer, Dordrecht, The Netherlands.
- Letouzey R. (1968) *Etude phytogéographique du Cameroun*. Lechevalier, Paris, France.
- Letouzey R. (1985) *Notice de la carte phytogéographique du Cameroun au 1:500 000*. Institut de la Carte Internationale de la Végétation, Toulouse, France.
- Levin N. E., Zipser E. J. and Cerling T. E. (2009) Isotopic composition of waters from Ethiopia and Kenya: insights into moisture sources for eastern Africa. *J. Geophys. Res.* **114**, D23306. doi:10.1029/2009JD012166.
- Mayaux P., Richards T. and Janodet E. (1999) A vegetation map of Central Africa derived from satellite imagery. *J. Biogeogr.* **26**, 353–366.
- McDermott F. (2004) Palaeo-climate reconstruction from stable isotope variations in speleothems: a review. *Quat. Sci. Rev.* **23**, 901–918.
- McInerney F. A., Helliker B. R. and Freeman K. H. (2011) Hydrogen isotope ratios of leaf wax *n*-alkanes in grasses are insensitive to transpiration. *Geochim. Cosmochim. Acta* **75**, 541–554.
- Meyers P. A. (2003) Applications of organic geochemistry to paleolimnological reconstructions: a summary of examples from the Laurentian Great Lakes. *Org. Geochem.* **34**, 261–289.
- Mügler I., Sachse D., Werner M., Xu B., Wu G., Yao T. and Gleixner G. (2008) Effect of lake evaporation on δD values of lacustrine *n*-alkanes: a comparison of Nam Co (Tibetan Plateau) and Holzmaar (Germany). *Org. Geochem.* **39**, 711–729.
- Mulch A., Graham S. A. and Chamberlain C. P. (2006) Hydrogen isotopes in Eocene river gravels and paleoelevation of the Sierra Nevada. *Science* **313**, 87–89.

- New M., Lister D., Hulme M. and Makin I. (2002) A high-resolution data set of surface climate over global land areas. *Climate Res.* **21**, 1–25.
- Nichols J., Booth R. K., Jackson S. T., Pendall E. G. and Huang Y. (2010) Differential hydrogen isotopic ratios of *Sphagnum* and vascular plant biomarkers in ombrotrophic peatlands as a quantitative proxy for precipitation–evaporation balance. *Geochim. Cosmochim. Acta* **74**, 1407–1416.
- Nicholson S. E. (2001) Climatic and environmental change in Africa during the last two centuries. *Climate Res.* **17**, 123–144.
- Niedermeyer E. M., Schefuß E., Sessions A. L., Multizzi S., Mollenhauer G., Schulz M. and Wefer G. (2010) Orbital- and millennial-scale changes in the hydrologic cycle and vegetation in the western African Sahel: insights from individual plant wax δD and $\delta^{13}\text{C}$. *Quat. Sci. Rev.* **29**, 2996–3005.
- Njitchoua R., Fontes J. C., Zuppi G. M., Aranyossy J. F. and Naah E. (1995) Use of chemical and isotopic tracers in studying the recharge of the upper Cretaceous aquifer of the Garoua basin, northern Cameroon. Application of Tracers in Arid Zone Hydrology, Proceedings of the Vienna Symposium, August 1994. IAHS Publ., No. 232, pp. 363–372.
- Olivry J. C. (1986) *Fleuves et rivières du Cameroun*. ORSTOM–MESRES, Paris.
- Pedentchouk N., Sumner W., Tipple B. and Pagani M. (2008) $\delta^{13}\text{C}$ and δD compositions of *n*-alkanes from modern angiosperms and conifers: an experimental set up in central Washington State, USA. *Org. Geochem.* **39**, 1066–1071.
- Poage M. A. and Chamberlain C. P. (2001) Empirical relationships between elevation and the stable isotope composition of precipitation and surface waters: considerations for studies of paleoelevation change. *Am. J. Sci.* **301**, 1–15.
- Polissar P. J. and Freeman K. H. (2010) Effects of aridity and vegetation on plant-wax δD in modern lake sediments. *Geochim. Cosmochim. Acta* **74**, 5785–5797.
- Rao Z., Zhu Z., Jia G., Henderson A. C. G., Xue Q. and Wang S. (2009) Compound specific δD values of long chain *n*-alkanes derived from terrestrial higher plants are indicative of the δD of meteoric waters: evidence from surface soils in eastern China. *Org. Geochem.* **40**, 922–930.
- Rommerskirchen F., Plader A., Eglinton G., Chikaraishi Y. and Rullkötter J. (2006) Chemotaxonomic significance of distribution and stable carbon isotopic composition of long-chain alkanes and alkan-1-ols in C_4 grass waxes. *Org. Geochem.* **37**, 1303–1332.
- Rowley D. B. and Garzione C. N. (2007) Stable isotope-based paleoaltimetry. *Annu. Rev. Earth Planet. Sci.* **35**, 463–508.
- Rozanski K., Araguás-Araguás L. and Gonfiantini R. (1993) Isotopic patterns in modern global precipitation. In *Climate Change in Continental Isotopic Records* (eds. P. K. Swart, K. C. Lohmann, J. A. McKenzie and S. Savin). Am. Geophys. Union, Washington, D.C., pp. 1–36.
- Russell J. M., McCoy S. J., Verschuren D., Bessem I. and Huang Y. (2009) Human impacts, climate change, and aquatic ecosystem response during the past 2000 yr at Lake Wandakara, Uganda. *Quat. Res.* **72**, 315–324.
- Sachs J. P. and Schwab V. F. (2011) Hydrogen isotopes in dinosterol from the Chesapeake Bay estuary. *Geochim. Cosmochim. Acta* **75**, 444–459.
- Sachse D., Radke J. and Gleixner G. (2004) Hydrogen isotope ratios of recent lacustrine sedimentary *n*-alkanes record modern climate variability. *Geochim. Cosmochim. Acta* **68**, 4877–4889.
- Sachse D., Radke J. and Gleixner G. (2006) δD values of individual *n*-alkanes from terrestrial plants along a climatic gradient – implications for the sedimentary biomarker record. *Org. Geochem.* **37**, 469–483.
- Sachse D., Kahmen A. and Gleixner G. (2009) Significant seasonal variation in the hydrogen isotopic composition of leaf-wax lipids for two deciduous tree ecosystems (*Fagus sylvatica* and *Acer pseudoplatanus*). *Org. Geochem.* **40**, 732–742.
- Sachse D., Gleixner G., Wilkes H. and Kahmen A. (2010) Leaf wax *n*-alkane δD values of field-grown barley reflect leaf water δD values at the time of leaf formation. *Geochim. Cosmochim. Acta* **74**, 6741–6750.
- Sauer P. E., Eglinton T. I., Hayes J. M., Schimmelmann A. and Sessions A. L. (2001) Compound-specific D/H ratios of lipid biomarkers from sediments as a proxy for environmental and climatic conditions. *Geochim. Cosmochim. Acta* **65**, 213–222.
- Schefuß E., Schouten S. and Schneider R. R. (2005) Climatic controls on central African hydrology during the past 20,000 years. *Nature* **437**, 1003–1006.
- Schimmelmann A., Lewan M. D. and Wintsch R. P. (1999) D/H isotope ratios of kerogen, bitumen, oil, and water in hydrous pyrolysis of source rocks containing kerogen types I, II, IIS, and III. *Geochim. Cosmochim. Acta* **63**, 3751–3766.
- Sessions A. L. (2006) Seasonal changes in D/H fractionation accompanying lipid biosynthesis in *Spartina alterniflora*. *Geochim. Cosmochim. Acta* **70**, 2153–2162.
- Sessions A. L., Burgoyne T. W., Schimmelmann A. and Hayes J. M. (1999) Fractionation of hydrogen isotopes in lipid biosynthesis. *Org. Geochem.* **30**, 1193–1200.
- Sinninghe Damsté J. S., Verschuren D., Ossebaar J., Blokker J., van Houten R., van der Meer M. T. J., Plessen B. and Schouten S. (2011) A 25,000-year record of climate-induced changes in lowland vegetation of eastern equatorial Africa revealed by the stable carbon-isotopic composition of fossil plant leaf waxes. *Earth Planet. Sci. Lett.* **302**, 236–246.
- Smith F. A. and Freeman K. H. (2006) Influence of physiology and climate on δD of leaf wax *n*-alkanes from C_3 and C_4 grasses. *Geochim. Cosmochim. Acta* **70**, 1172–1187.
- Still C. J. and Powell R. L. (2010) Continental-scale distributions of vegetation stable carbon isotope ratios. In *Isoscapes: Understanding Movement, Pattern, and Process on Earth Through Isotope Mapping* (eds. J. B. West, G. J. Bowen, T. E. Dawson and K. P. Tu). Springer, Dordrecht, The Netherlands, pp. 179–193.
- Suchel J. B. (1987) Les climats du Cameroun. Ph. D. thesis, Univ. Bordeaux III, France.
- Tanyileke G. Z., Kusakabe M. and Evans W. C. (1996) Chemical and isotopic characteristics of fluids along the Cameroon Volcanic Line, Cameroon. *J. Afr. Earth Sci.* **22**, 433–441.
- Tchoutou Mbatchou G. P. (2004) *Plant diversity in a Central African forest. Implications for biodiversity conservation in Cameroon*. Cameroon series, Tropenbos International, Wageningen, The Netherlands.
- Tierney J. E., Russell J. M., Huang Y., Sinninghe Damsté J. S., Hopmans E. C. and Cohen A. S. (2008) Northern hemisphere controls on tropical southeast African climate during the past 60,000 years. *Science* **322**, 252–255.
- Tierney J. E., Russell J. M., Sinninghe Damsté J. S., Huang Y. and Verschuren D. (2011) Late Quaternary behavior of the East African monsoon and the importance of the Congo Air Boundary. *Quat. Sci. Rev.* **30**, 798–807.
- van der Meer M. T. J., Schouten S., de Leeuw J. W. and Ward D. M. (2000) Autotrophy of green non-sulphur bacteria in hot spring microbial mats: biological explanations for isotopically heavy organic carbon in the geological record. *Environ. Microbiol.* **2**, 428–435.
- Vogts A., Moosse H., Rommerskirchen F. and Rullkötter J. (2009) Distribution patterns and stable carbon isotopic composition of alkanes and alkan-1-ols from plant waxes of African

- rain forest and savanna C₃ species. *Org. Geochem.* **40**, 1037–1054.
- Volkman J. K. (1986) A review of sterol markers for marine and terrigenous organic matter. *Org. Geochem.* **9**, 83–99.
- West A. G., Patrickson S. J. and Ehleringer J. R. (2006) Water extraction times for plant and soil materials used in stable isotope analysis. *Rapid Commun. Mass Spectrom.* **20**, 1317–1321.
- White, F. (1983) The Vegetation of Africa. A descriptive Memoir to Accompany the UNESCO/AETFAT/UNSO Vegetation Map of Africa. UNESCO, Paris, France.
- Xia Z. H., Xu B. Q., Mügler I., Wu G. J., Gleixner G., Sachse D. and Zhu L. P. (2008) Hydrogen isotope ratios of terrigenous *n*-alkanes in lacustrine surface sediment of the Tibetan Plateau record the precipitation signal. *Geochem. J.* **42**, 331–338.
- Zhang X. N., Gillespie A. L. and Sessions A. L. (2009) Large D/H variations in bacterial lipids reflect central metabolic pathways. *Proc. Natl. Acad. Sci. U. S. A.* **106**, 12580–12586.

Associate editor: Jaap S. Sinnenhe Damsté